



# A study on the EDM drilling of reaction-bonded silicon carbide using different electrode materials

Alexia Torres-Salcedo<sup>1</sup> · Carmelo Javier Luis-Pérez<sup>1</sup> · Ignacio Puertas-Arbizu<sup>1</sup> · Jesús María Corres-Sanz<sup>2</sup>

Received: 15 December 2022 / Accepted: 6 April 2023 / Published online: 28 April 2023  
© The Author(s) 2023

## Abstract

Today, there is a growing demand for efficient hole manufacturing technology in many industries such as aeronautics, automotive and nuclear, among others. Thus, the present study deals with the machining of through holes on SiSiC advanced ceramic by using Electrical Discharge Machining (EDM) drilling technology. Since recommendations related to the electrode characteristics and settings parameters are found to be scant for the industrial use of EDM drilling of SiSiC ceramics, this research work comes to cover this gap as it presents a complete study focused on the influence on different electrodes under rough and finish machining conditions. In particular, the influence of four electrodes materials (copper, copper-tungsten, graphite and copper infiltrated graphite) and three different electrode diameters ranging from 2 to 4 mm are investigated. In addition, the rotational speed of the electrode is also analysed. From the experimental results, both electrode material and machining regime, seem to be the most relevant factors of all. In the case of 2 mm diameter electrode, material removal rate (MRR) with Cu electrode was, approximately, 4.5 times higher than that obtained with a C electrode. In fact, it was found that copper electrode rotating at 20 rpm combined with high values of discharge energy ( $I=2$  A;  $t_i=70$   $\mu$ s) is the most economical option in terms of production cost and production time, as it gives a high MRR of 0.4754 mm<sup>3</sup>/min and a minimum electrode wear (EW) value of 7.52%. Moreover, slightly higher values of MRR were achieved for CuC electrode compared to those obtained with C electrode, indicating that the addition of Cu in the electrode contributes to a greater removal of material. However, a value of Ra of 0.37  $\mu$ m could be obtained by setting low current intensity values ( $I=0.5$  A;  $t_i=45$   $\mu$ s) combined with C electrodes and with no rotation.

**Keywords** EDM drilling · Through-hole · Electrode · Material removal rate · Surface roughness · Wear

## 1 Introduction

Nowadays, there is a growing demand for efficient hole manufacturing technology in many industries such as aeronautics, automotive and nuclear, among others. Components such as turbines blades [1], fuel injection nozzles [2], spinner holes [3] and bearings [4] are just a few examples of the most widely used products containing micro-holes. Moreover, moulding and assembly industries frequently require drilling of deep micro-holes in difficult-to-machine materials

[3]. In turn, many of these holed-components are usually made of hard ceramics materials that need high shape and dimensional accuracy.

Nowadays, advanced ceramics can offer many advantages over metals and polymer materials such as hardness, chemical inertness, thermal shock resistance, corrosion and wear resistance [5] and are more suitable for wear and high temperature applications due to their physical and chemical properties. In addition, they have replaced metals in applications involving reduced density and higher melting points [6] and are becoming more and more popular, not only in the tooling industry, but also in aerospace [7], biomedicine, armour and electronics industries [8]. Despite these excellent properties, one of their main drawbacks is their machining.

Most of the traditional machining techniques such as milling, turning or drilling would damage the surface of these advanced materials and they can produce cracks and stress concentration, which would affect the mechanical strength

✉ Ignacio Puertas-Arbizu  
inaki.puerta@unavarra.es

<sup>1</sup> Engineering Department, Public University of Navarre, Campus de Arrosadía s/n, 31006 Pamplona, Navarra, Spain

<sup>2</sup> Department of Electrical, Electronic and Communications Engineering, Public University of Navarre, Campus de Arrosadía s/n, 31006 Pamplona, Navarra, Spain

of the components [9]. In addition, the high cutting force achieved during their machining can cause premature tool wear [10], a longer process time and higher costs [11]. For these reasons, traditional methods do not seem the most suitable for their machining. Hence, the main goal of the manufacturing of advanced ceramic parts is how to obtain easy and low-cost effective processing techniques.

Electrical Discharge Machining (EDM) is one of the non-traditional methods most used for machining difficult-to-cut materials and for achieving, at the same time, the dimensional and geometrical performances required by the industry [12]. As it is a non-contact material removal method, any conductive material can be machined regardless of its hardness.

However, EDM requires machined materials to be conductive with a maximum electrical resistivity of 100–300  $\Omega\text{cm}$  [13]. Just as with metals, advanced conductive ceramics such as zirconium diboride ( $\text{ZrB}_2$ ), boron carbide ( $\text{B}_4\text{C}$ ), titanium diboride ( $\text{TiB}_2$ ), zirconium nitride ( $\text{ZrN}$ ) and titanium nitride ( $\text{TiN}$ ) can be performed by traditional EDM, but the machining of semiconductor and non-conductive advanced ceramics presents a great challenge [9].

Along these lines, silicon carbide (SiC), a very promising advanced ceramic, has a very high electrical resistivity of  $10^3$  to  $10^5$   $\Omega\text{cm}$ , which makes it difficult for EDM [14]. To enhance the EDM process of this ceramic, the infiltration of free Si into the SiC bulk material is presented as one of the most common techniques since it allows its electrical resistivity to be reduced down to 10  $\Omega\text{cm}$ , without affecting the mechanical properties of the material [15]. However, new techniques can be found in the literature such as those proposed by [16] and [17]. The first one suggests increasing the temperature of Si wafers to increase, in turn, their electrical conductivity. On the other hand, the second technique makes it possible to improve the conductivity of Si by means of a previous coating of Si with a high conductive metal such as gold.

## 2 State of the art

Recently, EDM drilling has become widely used in making holes in advanced ceramics. In fact, research is mainly focused on two aspects. On the one hand, on the analysis of the machining performance indicators such as material removal rate, tool wear ratio and surface roughness and, on the other hand, on the development of new models and machining strategies in order to improve and optimize the EDM drilling process.

As regards the performance of EDM drilling, the process parameters selected are crucial to achieving a high material removal rate and low tool wear ratios [18]. As EDM is a thermal process, its performance is essentially based on the

electrical parameters: current intensity, pulse time and open-circuit voltage as well as on tool polarity, flushing pressure and electrode material, among others. All these parameters can affect not only the rates of the material removed and the electrode wear, but they can also have a great influence on the properties of the machined part in terms of surface finish and geometrical and dimensional accuracy [19]. Because of this, many studies have been carried out for the optimization of the EDM drilling process.

Regarding electrical parameters, Clijsters et al. [14] examined the influence of discharge current, open gap voltage, discharge duration and pulse interval on machining performances like material removal rate, tool wear ratio and surface roughness of an EDM'ed SiSiC ceramic. Experimental results resulted in unstable machining when high energetic settings were selected whereas surface quality was improved by selecting relaxation pulses with low energy input. Furthermore, Yongfeng et al. [20] investigated the influence of EDM parameters including polarity of electrode, peak current, pulse-on time and pulse-off time on  $\text{ZrB}_2$ -SiC ceramics EDM machining process. Results were evaluated on material removal rate, side gap and surface roughness and the morphology and composites of machined surface were analysed by Scanning Electron Microscopy (SEM). Main conclusions included larger molten drops on the surface when the part was connected to anode and polygonal material layer and cylindrical flat areas when it was connected to cathode. On the other hand, Guu et al. [21] compared conventional EDM and rotary EDM on material removal rate and surface roughness on an AISI D2 tool steel with a copper electrode. In order to do that, the effects of pulsed current, pulse on-time and rotation were studied. Experimental results showed an increase in both material removal rate and surface roughness using electrode rotation due to an improvement in dielectric flow, which effectively helped remove debris from the gap between the electrode and the part. Finally, the influence of EDM drilling process parameters such as pulse duration, polarity and ignition voltage on material removal rate (MRR), electrode wear, machining time and hole diameter was studied by Kliuev et al. [22]. The highest rates of SiSiC material were found with negative polarity at 120 V and a pulse duration lower than 1  $\mu\text{s}$  whereas the lowest electrode wear was reached with positive electrode polarity and pulse duration of 5  $\mu\text{s}$ . Moreover, experiments showed almost linear dependence between ignition voltage and MRR in the range from 60 to 120 V and square law dependence between pulse duration and electrode wear in the range from 0.6 to 5  $\mu\text{s}$ .

The effects of machining conditions of EDM milling on the MRR, electrode wear ratio (EWR), and surface roughness (SR) of a SiC ceramic were investigated by Ji et al. [23]. To do so, three different machining conditions, namely

coarse machining, medium machining and fine machining, were applied and cylindrical copper electrodes were used. An increase in MRR and SR and a decrease in EWR from fine machining to coarse machining regardless of the tool polarity was observed. Moreover, the higher rates of MRR were obtained with negative tool polarity whereas the finer surface was found with positive tool polarity under the same conditions.

With respect to electrode, several studies can be found in the bibliography such as that from Gao [24], in which the influence of brass electrode length on the EDM tilted hole drilling process of kPa N5 superalloy was investigated. It was found that faster drilling speed occurred with the short electrode rather than with the long one because of pressure variation. The pressure loss of the short electrode was less than the longer electrode, especially for large length-diameter ratio electrode; thereafter, this could promote efficiency of flushing, thus resulting in higher drilling speed. Li et al. [25] used micro-electrical discharge machining in order to drill ZrB<sub>2</sub>-SiC-graphite composite. Cylinder and sheet electrodes were used and compared in terms of material removal rate and surface roughness. It was found that the use of sheet electrode led to a more stable process and the machining efficiency increased by 3.9 times on average compared with the cylinder shape electrode. Conversely, the machined surface became rougher and the widths of micro-cracks increased. Risto et al. [26] investigated the influence of electrode diameter and discharge energy on the geometrical accuracy and productivity of a 2.0 mm diameter borehole machined by EDM drilling. Experiments were conducted using four different tool electrode diameters which ranged from 1.6 to 1.9 mm. It was observed that the lowest cylindricity deviation occurred when using high discharge current values compared to higher discharge time.

With regard to the EDM drilling technique, many attempts have been made by earlier researchers to propose different methods for making holes by EDM. However, these techniques can be, in many cases, expensive or difficult to carry out. For example, Diver et al. [27] developed a new method to produce reverse tapered micro-holes on hardened steel flat plates with 1 mm thickness by using EDM. This method was based on feeding and rotating the electrode at the angle required in order to achieve the desired hole. The resulting holes could reach 100 µm diameter at electrode entry and 160 µm diameter at electrode exit. Furthermore, with this new method, it was also possible to improve the shape and diameter of conventional holes and to eliminate the neck effect that occurs during EDM drilling. Similar to this study, Bamberg et al. [28] made also the electrodes rotate so as to get micro-holes on a 316 stainless steel part by conventional EDM. Their experimental results showed holes with better surface finish, a decrease in electrode wear and faster machining

times as a result of an improved flushing. Yamazaki et al. [29] developed a novel technique to machine electrodes by using EDM drilling. This technique consisted of two steps: first of all, the tool electrode is rotated inside the part to obtain a hole. Then, the polarity is reversed, and it is the part itself that acts as an electrode to give the initial electrode the desired shape. This method allows the machining of electrode tools without the need to hold or position the electrode of the tool relative to that of the part.

In order to improve drilling time and surface roughness during deep-hole EDM drilling of an Inconel 718 part, Tanjilul et al. [30] proposed an efficient debris removal system based on simultaneously flushing and vacuum. To do so, a computational fluid dynamics model was proposed and the influence of debris particle size and EDM particle trajectory model were studied. Results indicated better surface roughness in the case of the use of vacuum-assisted drilling and larger size of debris particles with increasing machining current.

Li et al. [31] proposed a self-adjusting high speed drilling technology by using both EDM and Electro-Chemical Machining (ECM): EDM for drilling holes and ECM for removing recast layer. Moreover, internal and external flushing removal systems and dynamic change of discharge parameters were also proposed. This method allowed the material removal process to be adjusted based on gap distance and on hole-drilled depth. Experimental results, at different discharge parameters and using the new flushing systems, led to an improvement in discharge gap status and to a better flow of the working fluid.

Another machining strategy for the EDM of conductive ceramic materials such as B<sub>4</sub>C, SiSiC and WC-Co was developed by Luis et al. [32]. Design of Experiments (DOE) was employed as well as multiple linear regression techniques to get technological tables in order to programme die-sinking EDM machine-tools. Two different machining strategies (the first minimized the electrode wear and the second maximized the material removal rate) were used so as to obtain a specific surface roughness on the parts to be EDM'ed.

However, most of these studies refer to metals or metallic alloys and the literature available indicates a dearth of information regarding hole machining for advanced ceramic component application subjected to aggressive operating conditions. In fact, manufacturing industries are facing challenges in machining these advanced materials in terms of machining processes as well as machining costs [33].

Thus, this study aims to improve EDM drilling technique on conductive SiSiC ceramic by focusing on the factors that have been considered the most important and by optimizing machining conditions. For the industrial use of EDM drilling, there are no recommendations concerning the electrode material, diameter and machining settings for the discharge

energy to achieve a specific diameter [26]. Therefore, the main novelty of this research work lies in covering the above-mentioned gap.

### 3 Set-up of the experimentation

In the present section, the materials and the equipment used to conduct all the experiments are outlined first. Then, process performance variables as well as machining conditions are carefully described.

#### 3.1 Materials and equipment

Experiments were carried out on reaction-bonded silicon carbide plates with a 4 mm thickness. Its manufacturing process consisted in the infiltration of silicon into a preformed block of carbon and silicon carbide powder, which was subsequently subjected to a firing process. This produced around 10% of free silicon, which filled the pores and resulted in a low porosity microstructure and a very fine grain [34]. SiSiC has a high strength up to 1350 °C which results in its use as high temperature gas turbine components. In addition, it has a hardness higher than tungsten carbide which makes it possible for it to be used for bearings and seals. The high thermal conductivity (150–200 W/mK, at 20 °C) combined with low thermal expansion ( $4.3\text{--}4.6\cdot 10^{-6}\text{ K}^{-1}$ , at 20–1000 °C) leads to good thermal shock resistance [34]. SiSiC can tolerate a wider range of acids and alkalis than either tungsten carbide (WC) or alumina ( $\text{Al}_2\text{O}_3$ ). Moreover, the electrical resistivity of SiSiC is 10  $\Omega\text{cm}$  [14].

Since tool material has a great influence on EDM performance, four different electrode materials were chosen: copper (Cu), copper tungsten (CuW), graphite (C) and copper infiltrated graphite (CuC). All these materials have a high melting point and excellent thermal and electrical conductivities and were selected in order to have a wide

range of physical properties available: electrical resistivity, density and melting point. In addition, electrode diameter ranged from 2 to 4 mm. EDM holes were performed on a die-sinking electrical discharge machine ONA DATIC D-2030-S to which a drilling chuck was attached as shown in Fig. 1. Lateral flushing with a pressure of 80 kPa was used and mineral oil was selected as a dielectric fluid.

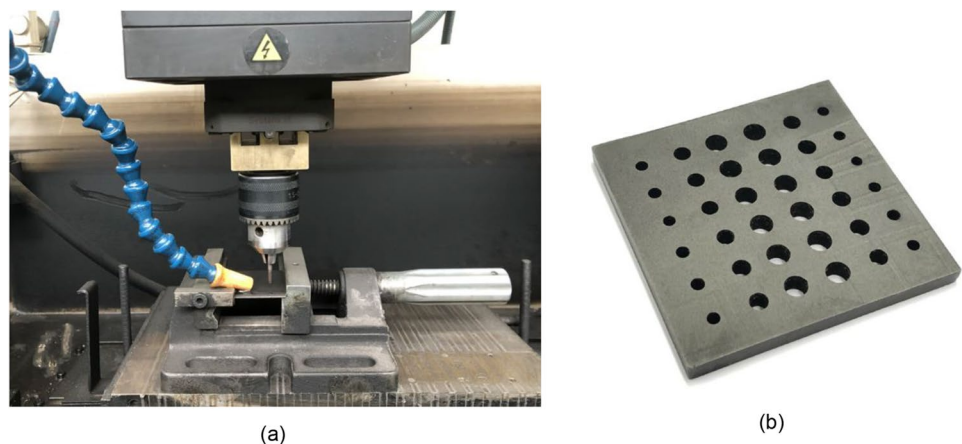
Both the part and electrode weights were measured before and after each experiment. Three measurements of each were carried out and then, the arithmetic mean was calculated. In order to do that, an electronic weighing scale Mettler Toledo XS 104 with a precision of ( $0.04\text{ mg} + 2\cdot 10^{-7}\cdot \text{weight}$ ) was used. In addition, the inlet and the outlet diameters of each experiment were also measured with an optical comparator at a magnification of  $20\times$ . Three measurements were taken and then, the arithmetic mean, as well as the standard deviation, were calculated.

Surface roughness was evaluated in terms of arithmetic mean roughness (Ra) as this is considered the most widely used parameter in the industry. This parameter is defined in UNE-EN ISO 4287:1999 [35]. In order to measure Ra, an ALPA SM-Rt-70 profile rugosimeter was employed.

Previously, the EDM drilled parts were sectioned into several pieces through the centre of the holes by using a copper sheet electrode as can be seen in Fig. 2. Then, every hole was measured at five different generatrices, equally distributed between the two halves; two on one half and three on the other half. Figure 3 shows the measurement technique. In all cases, each measurement was carried out for an evaluation length of 1.25 mm ( $5\times 0.25\text{ mm}$ ), 0.25 mm being the cut-off value and 5, the number of sampling lengths selected. In addition, a Gaussian filter was selected.

Finally, the image of each half hole was captured from the top of the piece using a Confocal S Mart microscope (Sensorfar) as shown in Fig. 4. Then, the edge of every experiment was characterized.  $5\times$  magnification was selected. Moreover,

**Fig. 1** EDM drilling process (a) and hole-drilled SiSiC (b)





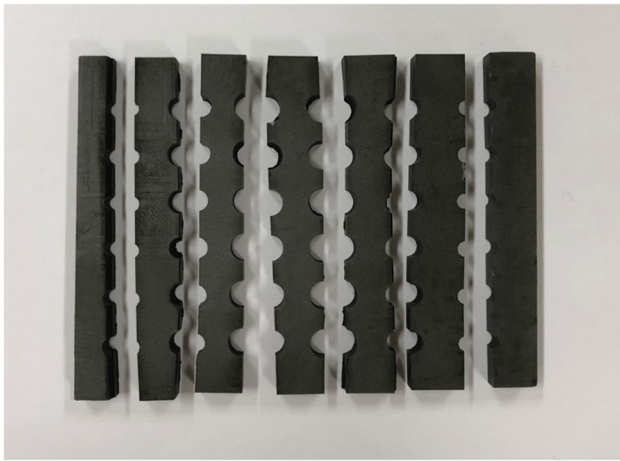


Fig. 2 Sectioned drilled part

this microscope enables vertical resolution of 75 nm to be obtained and a maximum slope of 8°.

### 3.2 Process performance

Process performance was evaluated in terms of MRR and electrode wear (EW). MRR ( $\text{mm}^3/\text{min}$ ) represents the efficiency of the EDM process and can be determined as the volume of material removed from part per minute as shown Eq. (1). On the other hand, EW (%) indicates the electrode loss ratio of EDM process and can be obtained according to Eq. (2), where  $\Omega_p$  and  $\Omega_e$  are the volume removed from the part and the electrode respectively, and  $t_m$  is the machining time.

$$\text{MRR} = \Omega_p / t_m \quad (1)$$

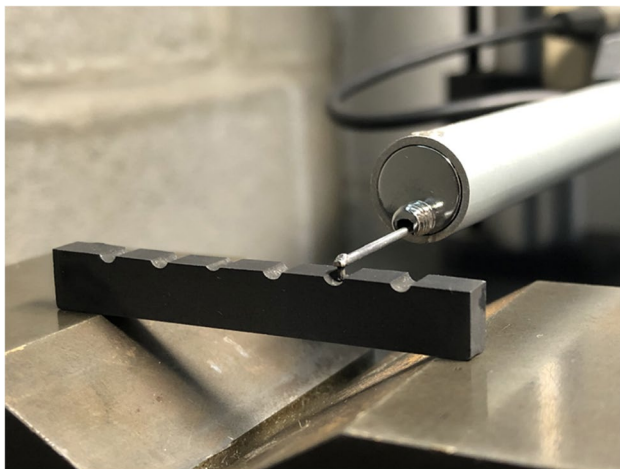


Fig. 3 Measurement technique

$$\text{EW} = (\Omega_e / \Omega_p) * 100 \quad (2)$$

In order to investigate the machining performance and surface roughness of EDM drilling of SiSiC ceramic profoundly, holes were drilled in several machining conditions. These conditions may be classified into the following: the first and the second are the electrode material and the electrode diameter, which directly influences both the EDM performance and surface roughness. The third one refers to the rotational speed of the electrode and it is related to the debris cleaning during the process. Finally, the last one is focused on EDM machining parameters such as current intensity ( $I$ ), pulse time ( $t_i$ ) and duty cycle ( $\eta$ ). Their values will define the machining regime. These three EDM machining parameters have been selected as they are the most important and the most common when selecting the amount of energy that is required to be used.

Table 1 shows the values of all the parameters selected. Since machining characteristics are quite different from those of metals and metallic alloys, previous tests had to be carried out to find out the optimal and stable machining conditions for SiSiC ceramic. Thus, for each electrode, a specific combination of parameters was set based on these preliminary studies.

Moreover, it should be noted that the maximum current intensity value selected is conditioned by the electrode section. According to the EDM machine manufacturer recommendations, in the case of metallic materials, this value must not exceed  $10 \text{ A/cm}^2$ . However, in the case of ceramic materials, this value may be higher due to

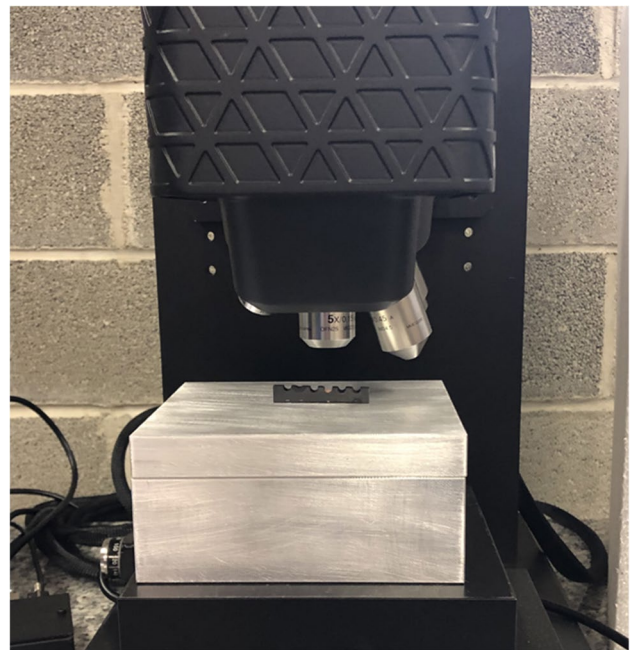


Fig. 4 Confocal microscope

**Table 1** Parameters combination for each electrode material

Electrode material	Electrode diameter (mm)	Rotational speed (rpm)	Regime					
			Roughing			Finishing		
			<i>I</i> (A)	<i>t<sub>i</sub></i> (μs)	<i>η</i> (%)	<i>I</i> (A)	<i>t<sub>i</sub></i> (μs)	<i>η</i> (%)
Copper (Cu)	2	0, 20, 40	1	70	0.6	0.5	50	0.5
	3	0, 20, 40	2	70	0.6	1	50	0.5
	4	0, 20, 40	2	70	0.6	1	50	0.5
Copper tungsten (CuW)	2	0, 20, 40	1	70	0.6	0.5	50	0.5
	3	0, 20, 40	2	70	0.6	1	50	0.5
	4	0, 20, 40	2	70	0.6	1	50	0.5
Graphite (C)	2	0, 20, 40	1	5	0.4	0.5	50	0.6
	3	0, 20, 40	2	5	0.4	1	50	0.6
	4	0, 20, 40	2	5	0.4	1	50	0.6
Graphite infiltrated copper (CuC)	2	0, 20, 40	1	5	0.4	0.5	50	0.6
	3	0, 20, 40	2	5	0.4	1	50	0.6
	4	0, 20, 40	2	5	0.4	1	50	0.6

their much lower conductivity. As can be seen, current intensity values were 0.5 A, 1 A, and 2 A. Although there are different current intensity pulses, the EDM machine used to conduct all the experiments generates square-wave diagrams. In line with this, the research study by Sánchez et al. [36] is worth mentioning, where an oscilloscope was connected to the EDM machine in order to obtain the actual values of the discharge current. These authors showed discharge current patterns in the conditions of maximum removal rate for the die-sinking EDM of the ceramic materials B<sub>4</sub>C and SiSiC.

Therefore, in order to obtain the actual values of current intensity and pulse time in this present study, an oscilloscope was also connected to the EDM machine. In all experimental cases, the values for the electrical parameters which were programmed in the generator of the EDM machine coincided with the actual ones. As an example, Figs. 5 and 6 show the waveform of both discharge current and voltage in both machining conditions: roughing (*I* = 2 A, *t<sub>i</sub>* = 5 μs, *η* = 0.4) and finishing (*I* = 1 A, *t<sub>i</sub>* = 50 μs, *η* = 0.6), respectively, in the case of CuC electrodes with 4 mm diameter. As can be seen, both parameters fluctuate periodically, and square-wave diagrams are nearly plotted. The height of the square wave refers to the peak amperes and voltage and, the horizontal reference line indicates that no electric current is flowing. In addition, it can also be seen that the values of peak current and pulse time are approximately 2 A and 5 μs, respectively, for roughing conditions and 1 A and 50 μs for finishing conditions, so it is assumed henceforward that both real and programmed values are the same.

In addition, open-circuit voltage and flushing pressure variables were kept constant at 200 V and 80 kPa, respectively. For all the experiments, negative polarity was used because it has been experimentally found that a more stable process is achieved in relation to positive polarity.

## 4 Results

The average values and the standard deviation obtained for each of the response variables and for each electrode material selected in the present study are listed in Table 2 for MRR, in Table 3 for EW and, finally, in Table 4 for Ra.

As can be observed in Table 2, experimental results indicate that the highest value of MRR (E8\_CuW) is 0.4974 mm<sup>3</sup>/min and it was obtained with a CuW electrode, diameter of 3 mm and rotational speed of 20 rpm, while the lowest value of MRR (E4\_C) is 0.0206 mm<sup>3</sup>/min and it was obtained with C electrode, 2 mm diameter and without electrode rotation.

With regard to EW, the highest value (E4\_C) is 1006.54% and this was obtained with a C electrode, diameter of 2 mm and with no electrode rotation, while the lowest EW value (E14\_Cu) is 7.52% and this was obtained with a Cu electrode of 4 mm diameter and at a rotational speed of 20 rpm, as can be seen in Table 3.

It was found that the highest value (E14\_CuW) of Ra is 1.11 μm and it was obtained using a CuW electrode, a diameter of 4 mm and a rotational speed of 20 rpm, while the lowest value (E4\_C) is 0.37 μm and it was obtained with a C

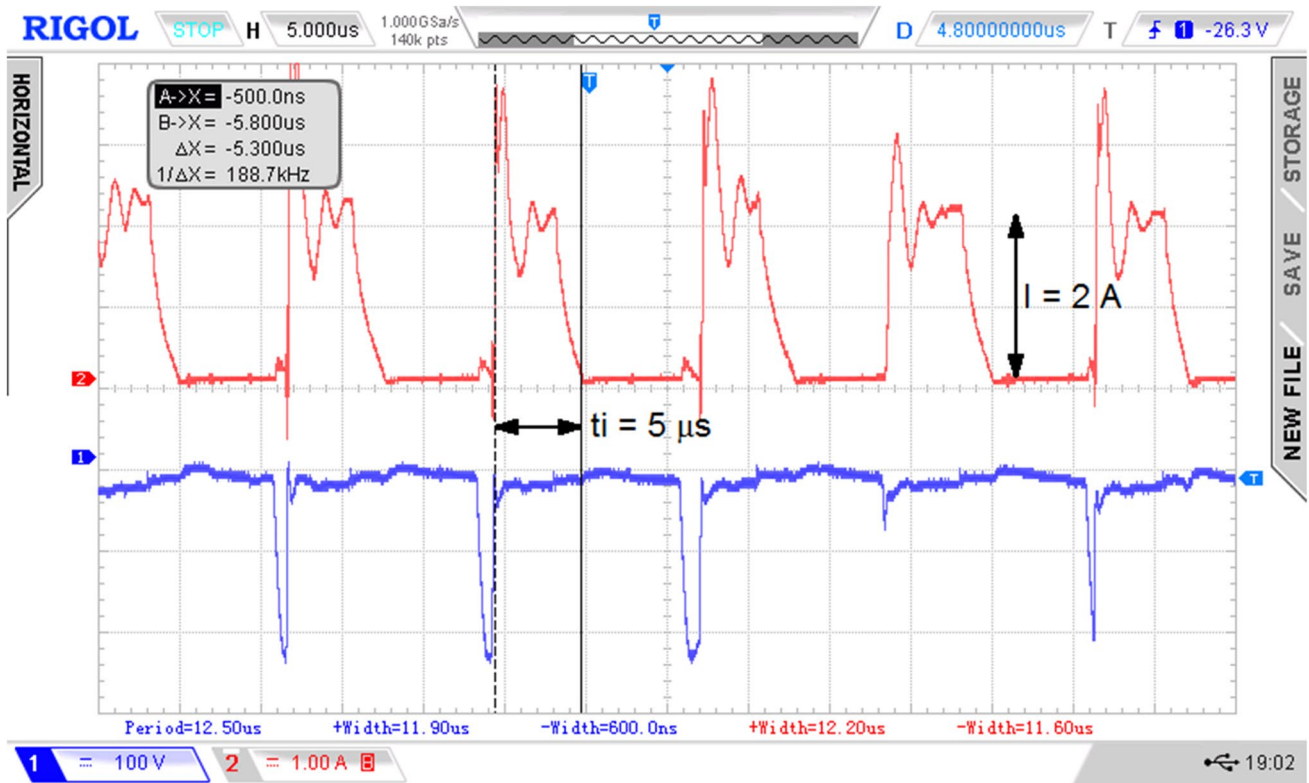


Fig. 5 Plot of current intensity and voltage patterns for CuC roughing conditions

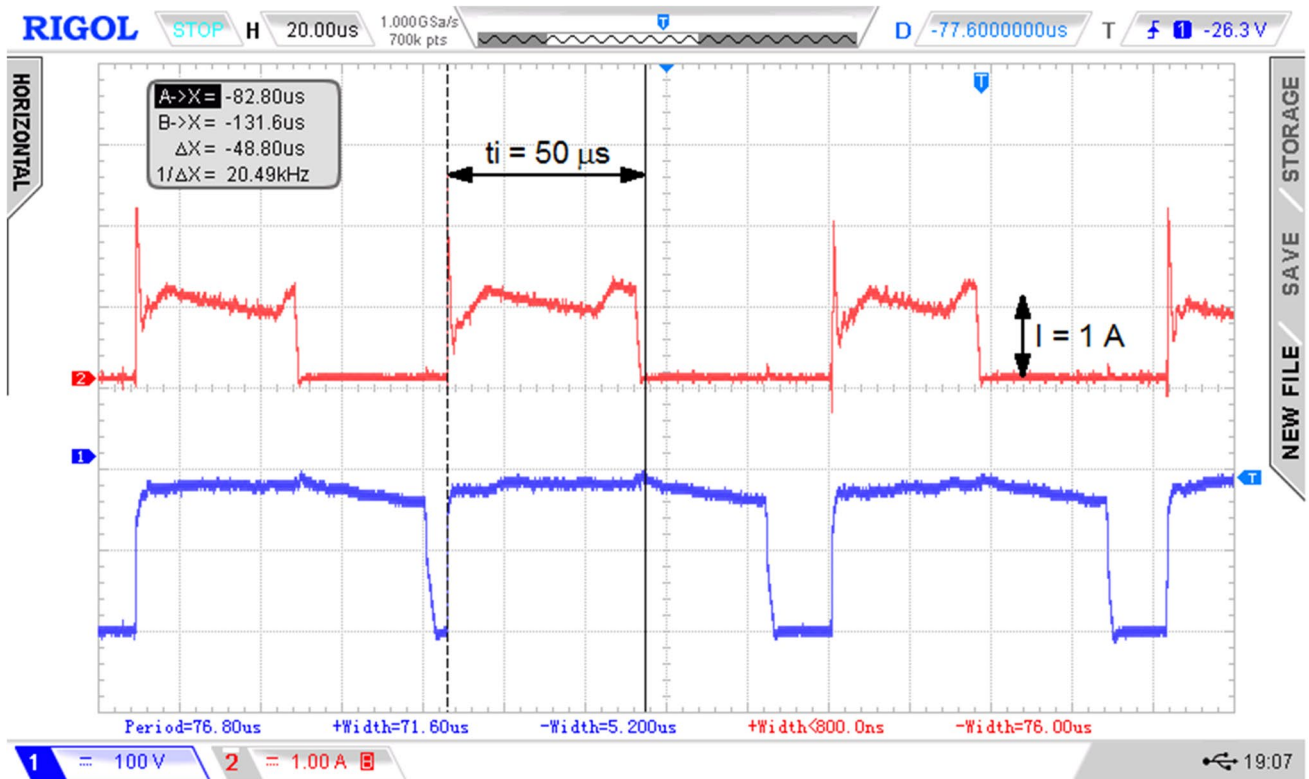


Fig. 6 Plot of current intensity and voltage patterns for CuC finishing conditions

**Table 2** MRR experimental results

E	Electrode diameter (mm)	Regime	Rotational speed (rpm)	MRR (mm <sup>3</sup> /min)			
				Cu	CuW	C	CuC
1	2	Roughing	0	0.0406 ± 0.0002	0.0323 ± 0.0001	0.0338 ± 0.0001	0.0384 ± 0.0001
2			20	0.2694 ± 0.0003	0.2268 ± 0.0003	0.0598 ± 0.0001	0.0687 ± 0.0002
3			40	0.2279 ± 0.0007	0.1483 ± 0.0007	0.0561 ± 0.0001	0.0670 ± 0.0001
4		Finishing	0	0.0430 ± 0.0001	0.0375 ± 0.0004	0.0206 ± 0.0001	0.0262 ± 0.0001
5			20	0.1528 ± 0.0002	0.1198 ± 0.0008	0.0269 ± 0.0001	0.0306 ± 0.0001
6			40	0.1181 ± 0.0007	0.0987 ± 0.0002	0.0418 ± 0.0001	0.0545 ± 0.0001
7	3	Roughing	0	0.2513 ± 0.0006	0.1793 ± 0.0003	0.0731 ± 0.0001	0.0888 ± 0.0005
8			20	0.4754 ± 0.0003	0.4974 ± 0.0007	0.0849 ± 0.0002	0.1501 ± 0.0003
9			40	0.3685 ± 0.0010	0.4349 ± 0.0007	0.0841 ± 0.0001	0.1403 ± 0.0001
10		Finishing	0	0.0746 ± 0.0003	0.0511 ± 0.0001	0.0478 ± 0.0001	0.0608 ± 0.0001
11			20	0.1395 ± 0.0002	0.1314 ± 0.0003	0.0481 ± 0.0001	0.0683 ± 0.0001
12			40	0.1123 ± 0.0001	0.1012 ± 0.0002	0.0660 ± 0.0001	0.0909 ± 0.0001
13	4	Roughing	0	0.2047 ± 0.0002	0.1707 ± 0.0001	0.1007 ± 0.0001	0.1083 ± 0.0001
14			20	0.3277 ± 0.0004	0.3096 ± 0.0002	0.1723 ± 0.0001	0.1810 ± 0.0004
15			40	0.2900 ± 0.0002	0.2848 ± 0.0003	0.1465 ± 0.0001	0.1788 ± 0.0001
16		Finishing	0	0.0616 ± 0.0001	0.0504 ± 0.0001	0.0503 ± 0.0001	0.0571 ± 0.0001
17			20	0.0959 ± 0.0001	0.1204 ± 0.0001	0.0866 ± 0.0001	0.0799 ± 0.0001
18			40	0.0725 ± 0.0001	0.0691 ± 0.0001	0.1089 ± 0.0001	0.0903 ± 0.0001

electrode of 2 mm diameter and with no electrode rotation, as shown in Table 4.

Finally, Tables 5 and 6 show the mean and the standard deviation values of the inlet and the outlet diameters for each

experiment as well as taper angles, respectively. The taper angle was measured as the difference between the inlet diameter and the outlet diameter of the hole according to Eq. (3), where  $h$  is the thickness of the part that was 4 mm.

**Table 3** EW experimental results

E	Electrode diameter (mm)	Regime	Rotational speed (rpm)	EW (%)			
				Cu	CuW	C	CuC
1	2	Roughing	0	31.49 ± 0.07	31.87 ± 0.13	396.86 ± 0.48	193.43 ± 0.43
2			20	12.81 ± 0.16	15.69 ± 0.08	285.69 ± 0.26	178.43 ± 0.52
3			40	14.22 ± 0.06	28.29 ± 0.17	266.71 ± 0.61	153.98 ± 0.16
4		Finishing	0	23.69 ± 0.05	33.98 ± 0.43	1006.54 ± 2.06	778.83 ± 1.02
5			20	12.54 ± 0.12	13.04 ± 0.11	686.12 ± 1.34	716.36 ± 1.87
6			40	15.90 ± 0.23	20.91 ± 0.01	571.79 ± 0.54	607.23 ± 1.10
7	3	Roughing	0	17.62 ± 0.07	18.02 ± 0.05	306.67 ± 0.46	133.35 ± 0.38
8			20	11.12 ± 0.07	15.26 ± 0.02	246.37 ± 0.56	120.69 ± 0.34
9			40	13.54 ± 0.05	18.13 ± 0.09	230.80 ± 0.16	110.09 ± 0.11
10		Finishing	0	21.01 ± 0.07	27.80 ± 0.13	680.48 ± 0.58	702.06 ± 0.33
11			20	10.63 ± 0.16	11.96 ± 0.01	602.66 ± 0.69	440.33 ± 0.43
12			40	12.75 ± 0.06	16.86 ± 0.07	408.57 ± 0.60	431.24 ± 0.49
13	4	Roughing	0	13.94 ± 0.04	22.77 ± 0.05	350.40 ± 0.29	185.32 ± 0.13
14			20	7.52 ± 0.02	13.65 ± 0.02	269.47 ± 0.11	121.57 ± 0.08
15			40	9.16 ± 0.04	14.81 ± 0.04	258.24 ± 0.13	114.24 ± 0.06
16		Finishing	0	16.75 ± 0.08	17.77 ± 0.02	952.69 ± 1.26	777.17 ± 0.72
17			20	11.63 ± 0.02	7.55 ± 0.02	616.42 ± 0.48	532.47 ± 0.30
18			40	12.22 ± 0.05	11.71 ± 0.01	479.46 ± 0.21	502.41 ± 0.27



**Table 4** Ra experimental results

E	Electrode diameter (mm)	Regime	Rotational speed (rpm)	Ra (μm)			
				Cu	CuW	C	CuC
1	2	Roughing	0	0.75 ± 0.07	0.84 ± 0.02	0.59 ± 0.07	0.45 ± 0.05
2			20	0.90 ± 0.07	0.93 ± 0.10	0.68 ± 0.04	0.46 ± 0.01
3			40	0.77 ± 0.07	0.87 ± 0.08	0.60 ± 0.02	0.45 ± 0.05
4		Finishing	0	0.53 ± 0.03	0.51 ± 0.03	0.37 ± 0.05	0.37 ± 0.05
5			20	0.66 ± 0.04	0.60 ± 0.06	0.47 ± 0.04	0.39 ± 0.03
6			40	0.64 ± 0.04	0.51 ± 0.09	0.48 ± 0.03	0.40 ± 0.03
7	3	Roughing	0	0.68 ± 0.04	0.76 ± 0.12	0.59 ± 0.03	0.57 ± 0.03
8			20	0.83 ± 0.07	0.85 ± 0.04	0.82 ± 0.02	0.69 ± 0.06
9			40	0.71 ± 0.06	0.81 ± 0.06	0.63 ± 0.04	0.61 ± 0.02
10		Finishing	0	0.47 ± 0.05	0.69 ± 0.05	0.45 ± 0.04	0.45 ± 0.07
11			20	0.54 ± 0.03	0.83 ± 0.08	0.48 ± 0.04	0.54 ± 0.02
12			40	0.52 ± 0.04	0.79 ± 0.05	0.52 ± 0.03	0.54 ± 0.02
13	4	Roughing	0	0.88 ± 0.09	1.01 ± 0.07	0.56 ± 0.06	0.60 ± 0.08
14			20	1.07 ± 0.12	1.11 ± 0.14	0.65 ± 0.05	0.78 ± 0.11
15			40	0.98 ± 0.02	1.03 ± 0.04	0.58 ± 0.05	0.65 ± 0.05
16		Finishing	0	0.66 ± 0.06	0.50 ± 0.05	0.41 ± 0.04	0.47 ± 0.03
17			20	0.76 ± 0.08	0.72 ± 0.07	0.42 ± 0.02	0.51 ± 0.07
18			40	0.68 ± 0.03	0.55 ± 0.07	0.45 ± 0.05	0.57 ± 0.03

**Table 5** Electrode diameter and inlet and outlet hole diameters

E	Electrode diameter (mm)	Cu		CuW		C		CuC	
		Inlet diameter (mm)	Outlet diameter (mm)	Inlet diameter (mm)	Outlet diameter (mm)	Inlet diameter (mm)	Outlet diameter (mm)	Inlet diameter (mm)	Outlet diameter (mm)
1	2.00	2.21 ± 0.01	2.13 ± 0.01	2.20 ± 0.01	2.07 ± 0.02	2.13 ± 0.01	2.11 ± 0.01	2.22 ± 0.01	2.15 ± 0.01
2		2.39 ± 0.01	2.31 ± 0.01	2.26 ± 0.01	2.24 ± 0.01	2.33 ± 0.01	2.06 ± 0.01	2.40 ± 0.01	2.31 ± 0.01
3		2.33 ± 0.01	2.31 ± 0.01	2.28 ± 0.01	2.06 ± 0.01	2.36 ± 0.01	2.03 ± 0.01	2.38 ± 0.01	2.25 ± 0.02
4		2.23 ± 0.01	2.13 ± 0.01	2.09 ± 0.01	1.96 ± 0.01	2.36 ± 0.01	2.03 ± 0.01	2.27 ± 0.01	2.13 ± 0.01
5		2.39 ± 0.01	2.31 ± 0.01	2.34 ± 0.01	2.04 ± 0.01	2.35 ± 0.01	2.11 ± 0.01	2.41 ± 0.02	2.35 ± 0.01
6		2.28 ± 0.01	2.15 ± 0.01	2.27 ± 0.01	1.99 ± 0.01	2.31 ± 0.01	2.06 ± 0.01	2.29 ± 0.01	2.15 ± 0.01
7	3.00	3.26 ± 0.01	3.15 ± 0.01	3.25 ± 0.01	3.12 ± 0.01	3.17 ± 0.01	3.13 ± 0.01	3.23 ± 0.01	3.16 ± 0.01
8		3.24 ± 0.01	3.09 ± 0.01	3.25 ± 0.02	3.07 ± 0.02	3.33 ± 0.01	3.14 ± 0.01	3.22 ± 0.01	3.08 ± 0.01
9		3.14 ± 0.01	3.07 ± 0.01	3.17 ± 0.01	3.05 ± 0.01	3.29 ± 0.01	3.13 ± 0.01	3.13 ± 0.01	3.06 ± 0.01
10		3.08 ± 0.01	2.95 ± 0.01	3.05 ± 0.01	2.95 ± 0.01	3.24 ± 0.01	3.10 ± 0.01	3.05 ± 0.01	2.96 ± 0.01
11		3.21 ± 0.01	3.13 ± 0.01	3.20 ± 0.01	3.12 ± 0.01	3.49 ± 0.01	3.10 ± 0.01	3.18 ± 0.01	3.13 ± 0.01
12		3.21 ± 0.01	3.16 ± 0.02	3.22 ± 0.01	2.97 ± 0.01	3.31 ± 0.01	3.01 ± 0.01	3.19 ± 0.02	2.83 ± 0.01
13	4.00	4.27 ± 0.01	4.06 ± 0.01	4.05 ± 0.01	3.99 ± 0.01	4.11 ± 0.01	4.02 ± 0.01	4.06 ± 0.01	3.93 ± 0.01
14		4.35 ± 0.01	4.05 ± 0.02	4.34 ± 0.01	4.00 ± 0.01	4.23 ± 0.01	4.17 ± 0.01	4.21 ± 0.01	4.01 ± 0.01
15		4.30 ± 0.01	4.04 ± 0.02	4.30 ± 0.02	3.99 ± 0.01	4.20 ± 0.01	4.10 ± 0.01	4.14 ± 0.01	3.95 ± 0.01
16		4.34 ± 0.01	4.04 ± 0.01	4.35 ± 0.01	4.12 ± 0.02	4.07 ± 0.01	3.99 ± 0.01	4.12 ± 0.01	4.03 ± 0.01
17		4.32 ± 0.01	4.13 ± 0.01	4.34 ± 0.01	4.14 ± 0.01	4.18 ± 0.01	4.09 ± 0.01	4.05 ± 0.01	3.84 ± 0.01
18		4.22 ± 0.01	4.09 ± 0.01	4.28 ± 0.02	4.09 ± 0.02	4.12 ± 0.01	4.03 ± 0.01	4.04 ± 0.01	3.90 ± 0.01

**Table 6** Taper angle (°)

E	Electrode diameter (mm)	Cu	CuW	C	CuC
1	2.00	0.57	0.93	0.14	0.50
2		0.57	0.14	1.93	0.64
3		0.14	1.58	2.15	0.93
4		0.72	0.93	2.36	1.00
5		0.57	2.15	1.72	0.43
6		0.93	2.00	1.79	1.00
7	3.00	0.79	0.93	0.29	0.50
8		1.07	1.29	1.36	1.00
9		0.50	0.86	1.15	0.50
10		0.93	0.72	1.00	0.64
11		0.57	0.57	2.79	0.36
12		0.36	1.79	2.15	2.58
13	4.00	1.50	0.43	0.64	0.93
14		2.15	2.43	0.43	1.43
15		1.86	2.22	0.72	1.36
16		2.15	1.65	0.57	0.64
17		1.36	1.43	0.64	1.50
18		0.93	1.36	0.64	1.00

$$\text{Taper angle} = \tan^{-1} \frac{D_{\text{inlet}} - D_{\text{outlet}}}{2h} \quad (3)$$

As can be seen, in all cases the inlet diameter is slightly larger than the outlet diameter as a result of the wear suffered by the electrode during the EDM process. However, it should be noted that in 68% of the cases, this difference is less than 0.1 mm and there is no case higher than 0.2 mm. This confirms a high machining accuracy. The greatest differences found between both diameters correspond to 0.15 mm, 0.17 mm, 0.20 mm and 0.18 mm for Cu, CuW, C and CuC electrodes, respectively. Likewise, it is also observed that the value of all the standard deviations is very low, being, in general terms, 0.01 mm.

It can also be appreciated that, in some cases, the outlet diameter value is lower than the electrode diameter (2, 3 and 4 mm), where this fact indicates, again, that the electrode suffers wear during the EDM process.

Regarding taper angle, very low values are observed: approximately 84.7% of the cases have a taper angle less than 2°. In the case of Cu, CuW and CuC electrodes and for electrode diameters of 2 mm and 3 mm, lower conicity values are observed in comparison with 4 mm diameter electrode. Nevertheless, in the case of C electrode, the lowest values are observed for 4 mm diameter electrode.

## 5 Discussion of results

In this section, EDM drilling performance as well as surface roughness are analysed. In line with the structure followed in the planning of the experimentation, the analysis of results is focused, firstly, on the influence of electrode material, secondly, on the influence of the diameter and the rotational speed of the electrode and, finally, on the EDM regime by means of the variation of EDM parameters (current intensity, pulse time and duty cycle) on response variables MRR, EW and Ra.

To carry out this analysis, statistical techniques have been used. In fact, one interesting technique in order to draw conclusions from the data obtained is the comparison of mean values by the Fisher Least Significant Difference (LSD) Method [37]. With this method, a pair of mean values is considered to be significantly different if their difference is higher than a value which is called the least significant difference. In other words, if the observed difference between each pair of means is less than the calculated LSD value, it may be concluded that those means do not differ and that they cannot be considered to be different. If the design is balanced, which means that all the samples have the same number of observations ( $n$ ), this LSD value is calculated as can be observed in Eq. (4):

$$\text{LSD} = t_{\alpha/2, N-a} * \sqrt{(2 * MS_E/n)} \quad (4)$$

where  $t$  is the  $t$  distribution with  $N-a$  degrees of freedom.  $N$  is the total number of observations,  $n$  is the number of observations for each sample,  $a$  is the number of samples to compare and  $MS_E$  is the mean square due to error within means. In the plots that will be shown in this present research study, the LSD values to make the comparison analysis will be depicted as the length of the intervals.

Finally, it should be noted that similar trends have been found in the results obtained with the 2, 3 and 4 mm electrodes. For this reason, in order to simplify the number of figures, only the graphs that refer to the experiments carried out with 2 mm electrode have been introduced. In any case if there is any difference, it is detailed in the full text.

### 5.1 Material removal rate

Material removal rate was measured and compared for all electrode materials selected. In order to identify the materials whose means are statistically different, Fig. 7 reports the MRR mean data plot as a function of the electrode material. Error bars indicate the 95% confidence interval of the LSD

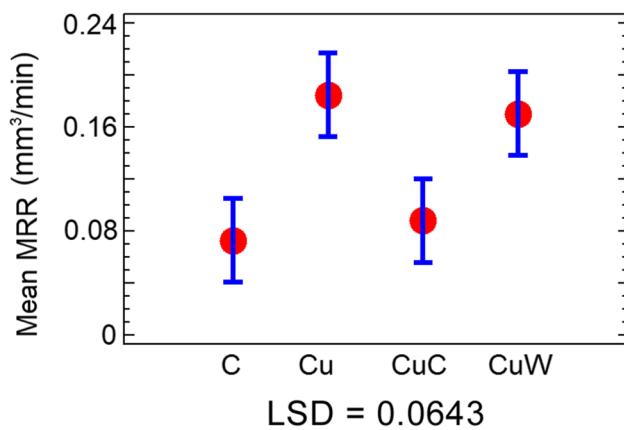


**Fig. 7** Results for Fisher's LSD mean comparisons for MRR vs. electrode material

mean. Furthermore, it should be noted that the LSD value, represented by the total length of the interval, is the same for each case. In the case of MRR, this value is 0.0643. As can be observed, results for C and CuC electrodes and for Cu and CuW electrodes are very similar in terms of machining speed because their corresponding LSD intervals are overlapped. However, significant differences can be found between the results of the two previous electrode materials and those of Cu and CuW (because their corresponding LSD intervals are not overlapped), which, in turn, constitute homogeneous groups between them. These results are due to the fact that the composition of each pair of materials is very similar, allowing the C and CuC electrodes to be grouped in the graphite group and the Cu and CuW electrodes to be grouped in the copper one.

Figure 8 shows mean data plot as a function of electrode diameter (a), rotational speed of the electrode (b), and machining regime (c) for all the material electrodes selected in this study. The main objective of this summary graph is to identify in a visual manner if significant differences can be found between the four electrode materials. Moreover, LSD value for each graph is detailed.

From Fig. 8(a), it can be noted that there are no significant differences for the different diameter values in the case of Cu and CuW. In the case of C and CuC, there are significant differences between the diameters of 2 mm and 4 mm, so that the speed machining values increase with the size of the hole diameter. This result is the expected one as previous experiences in EDM drilling with other materials indicate an increase in machining speed by increasing the machining surface for the same conditions [38]. Due to this area effect, the discharge energy of a single spark increases, and

the breakdown field strength decreases with the increase of tool electrode diameter. Therefore, the crater size of a single discharge and the discharge frequency increase, and MRR increases [39].

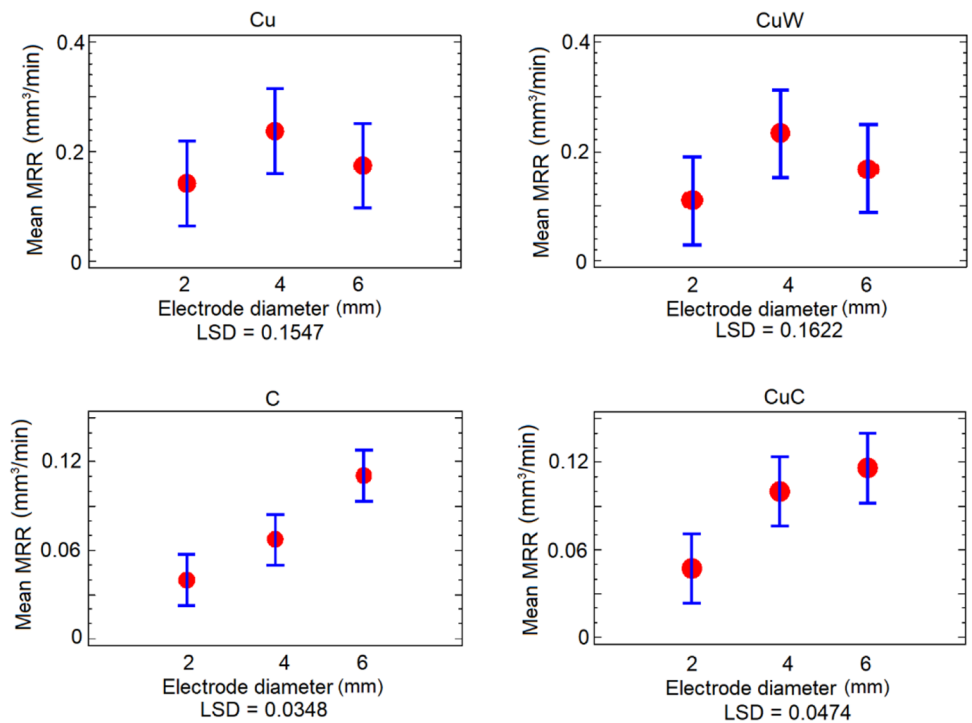
Regarding rotational speed of the electrode (see Fig. 8(b)), differences do not seem to be very relevant when it is varied from 20 to 40 rpm for any of the materials used. However, significant differences were found when varying the machining regime: the roughing regime always leads to a higher material removal for any electrode material, as can be seen in Fig. 8(c).

Figure 9 represents the relationship between the rotational speed of the 2 mm electrode and MRR at different electrode materials and machining regime.

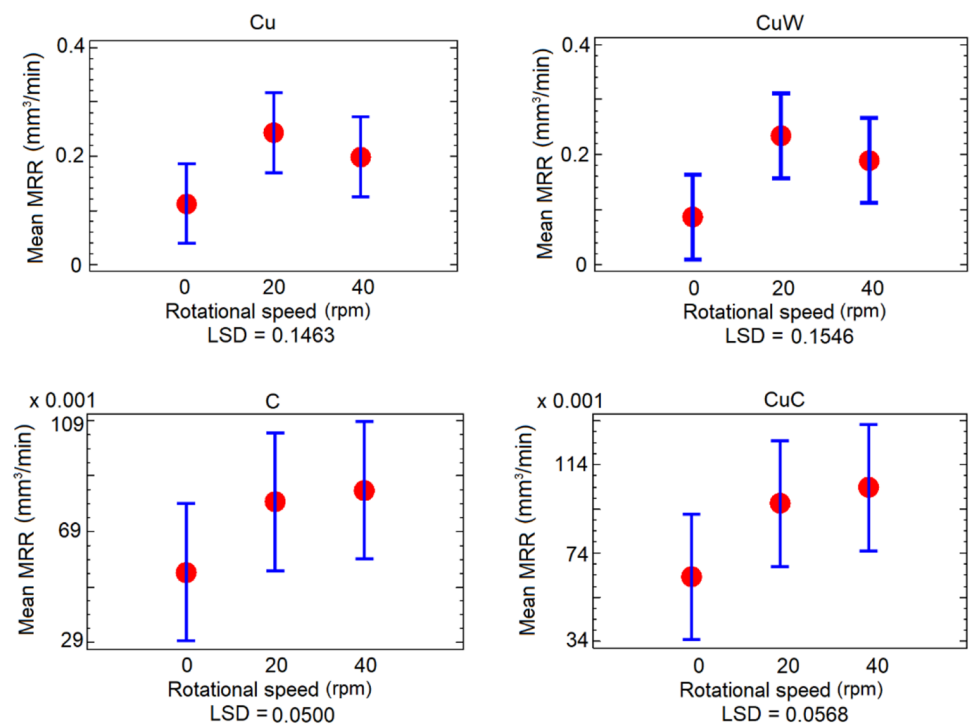
As can be observed, the electrode material has a relevant influence on MRR. In particular, higher MRR rates are obtained with Cu and CuW electrodes, both in finishing and roughing regimes for any electrode diameter. This is due to the comparatively lower electrical resistivity of Cu ( $1.7 \cdot 10^{-8} \Omega\text{m}$ ) and CuW ( $4.3 \cdot 10^{-8} \Omega\text{m}$ ) to that of C ( $19.3 \cdot 10^{-6} \Omega\text{m}$ ) and CuC ( $3.2 \cdot 10^{-6} \Omega\text{m}$ ) which allows a more stable and homogeneous process. Specifically, in roughing regime and at 20 rpm, the greatest removal rate is appreciated, whatever the diameter of the electrode. For example, as can be seen in Table 2, in the case of 2 mm diameter electrode, the material removal rate with a Cu electrode is, approximately, 4.5 times higher than that obtained with a C electrode (for Cu is  $0.2694 \text{ mm}^3/\text{min}$  and for C is  $0.0598 \text{ mm}^3/\text{min}$ ), with a diameter of 3 mm, it is 5.5 times higher (for Cu is  $0.4754 \text{ mm}^3/\text{min}$  and for C is  $0.0849 \text{ mm}^3/\text{min}$ ) and with a diameter of 4 mm is almost twice (for Cu is  $0.3277 \text{ mm}^3/\text{min}$  and for C is  $0.1723 \text{ mm}^3/\text{min}$ ).

With respect to rotational speed of the electrode, as can be observed in Fig. 9, with Cu and CuW electrodes, both in finishing and roughing regimes, the highest MRR rate is reached at 20 rpm. In such cases, the removal rate increases with increasing rotational speed up to a maximum (20 rpm), after which it begins to slightly decrease. In the case of C and CuC electrodes, in roughing regime there is no great MRR difference between rotational speeds of 20 rpm and 40 rpm. However, in finishing regime, as the rotational speed of the electrode increases, MRR also increases. Furthermore, it should be noted that slightly higher values of MRR were achieved for CuC electrode compared to those obtained with C electrode. For example, as shown Table 2, in roughing regime and for the three rotational speeds selected, values of  $0.0384 \text{ mm}^3/\text{min}$ ,  $0.0687 \text{ mm}^3/\text{min}$  and  $0.0670 \text{ mm}^3/\text{min}$  were achieved with CuC electrode, while values of  $0.0338 \text{ mm}^3/\text{min}$ ,  $0.0598 \text{ mm}^3/\text{min}$  and  $0.0561 \text{ mm}^3/\text{min}$ , respectively, were obtained with C electrode. In the case of

**Fig. 8** Results for Fisher's LSD mean comparisons for MRR vs. electrode diameter (a), rotational speed (b) and machining regime (c)



(a)



(b)

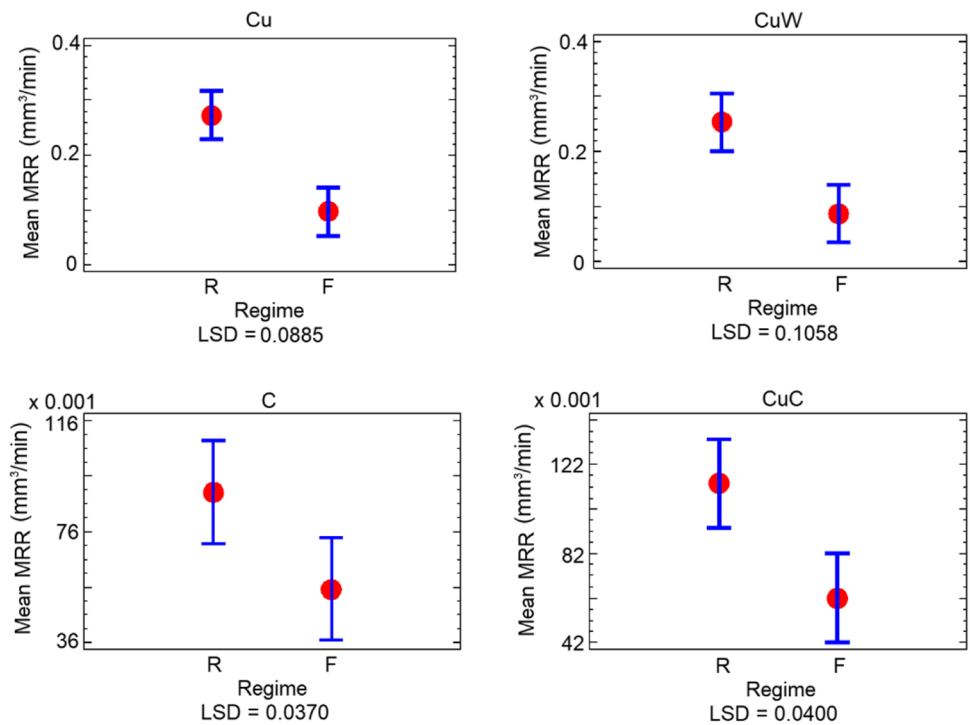
finishing regime, MRR values with CuC electrodes were: 0.0262 mm<sup>3</sup>/min, 0.0306 mm<sup>3</sup>/min and 0.0545 mm<sup>3</sup>/min and with C electrodes were: 0.0206 mm<sup>3</sup>/min, 0.0269 mm<sup>3</sup>/min and 0.0418 mm<sup>3</sup>/min. This fact indicates that the addition

of Cu in the C electrode contributes to a greater removal of material.

Since the rotational speed of the electrode is one of the major factors on the debris evacuation during EDM



Fig. 8 (continued)



(c)

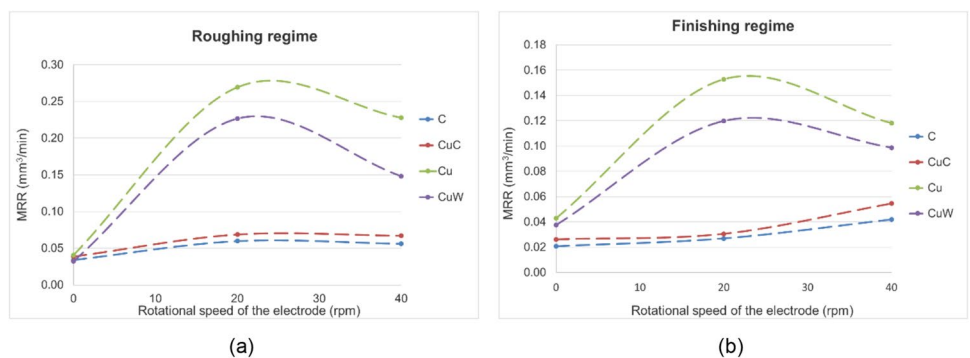
process, the highest MRR rates were achieved by rotating the electrode. This rotation allows the debris particles that can accumulate in the cavities and thus increase machining time to be evacuated and to be cleaned. From these obtained results, it has been observed that the beneficial effect of the electrode rotation reaches a maximum value at 20 rpm. From this point, a saturation effect takes place because of the appearance of turbulences, which implies even a little decrease in MRR.

Regarding machining regime, it is clearly observed that the highest removal rates were achieved in the roughing regime versus the finishing regime, regardless of the material, rotational speed and diameter of the electrode. This is mainly due to the higher intensity values selected. Thermal energy is provided through electricity flowing between the electrode and the part in the form of a spark.

During each spark, millions of electrons flow between the electrode and the part in a dielectric medium. When the electrons hit the part, they release their energy as heat, which vaporizes the material in the part. Amperes are used to denote the amount of electricity used in the machining process [40]. Thus, MRR increases significantly when current intensity increases due to an increase in the heat and in the energy that melts and vaporizes the material from the part.

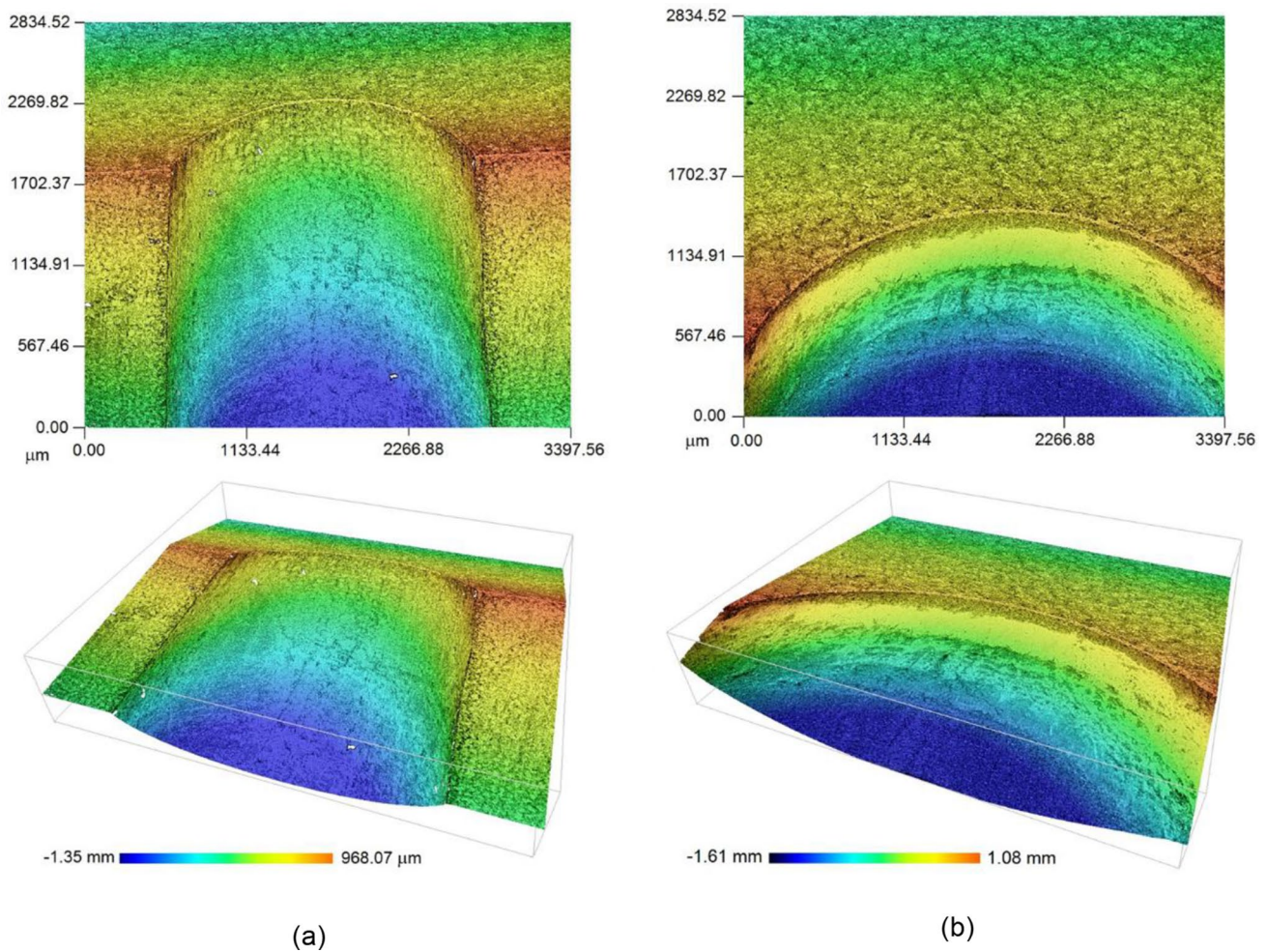
At low current, a small amount of heat is generated. A substantial part of this heat is absorbed by the environment and the components of the EDM machine and the remainder is used to melt and vaporize the part. But as the current increases, stronger sparks and more energy are produced, and a greater amount of heat is made available to remove the material [41].

Fig. 9 Effect of rotational speed on MRR at different electrode materials and working conditions (electrode diameter 2 mm)



(a)

(b)



**Fig. 10** Surface topography at the entrance of the hole at (a) maximum MRR (E8\_CuW) and (b) minimum MRR conditions (E4\_C)

In addition, microscope analysis is included to examine the surface quality of the hole, both of the edge and of the side walls. Thus, Fig. 10(a) and (b) shows the electrode entry hole of the experiment E8\_CuW corresponding to the maximum value of MRR ( $0.4974 \text{ mm}^3/\text{min}$ ) and of the experiment E4\_C corresponding to the minimum MRR value ( $0.0206 \text{ mm}^3/\text{min}$ ), respectively. As shown, Table 4 Ra values for both experiments were  $0.85 \text{ μm}$  and  $0.37 \text{ μm}$ , respectively. Moreover, these Ra values were compared to those obtained with the microscope. In this case, Ra values were  $1.01 \text{ μm}$  for E8\_CuW and  $0.49 \text{ μm}$  for E4\_C. As can be seen, both results are very similar.

According to Fig. 10, in both cases, the edges are very well defined and burr-free as there is little re-solidified material around the hole which avoids the use of secondary deburring-type operations. This results in a faster, more

efficient and economical manufacturing process. Moreover, this result can be attributed to the flushing cleaning and in this case, its corresponding dielectric pressure value ( $80 \text{ kPa}$ ) turned out to be adequate taking the edge surface topography obtained into account. Previous experiences in EDM drilling show that there is a direct influence of the dielectric flow rate in removal of the molten material near the discharge zone [42].

## 5.2 Electrode wear

With respect to electrode wear, Fig. 11 depicts the EW mean data plot as a function of the electrode material. As can be seen, the variation of the electrode material is clearly significant in its wear. In fact, the choice of electrode material not only affects MRR, as seen above, but also has a direct impact

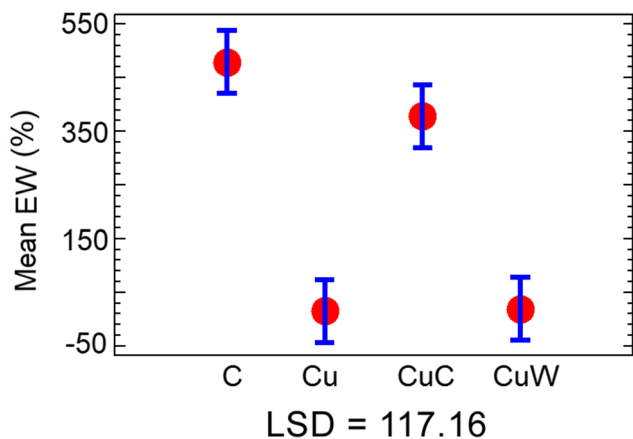


**Fig. 11** Results for Fisher’s LSD mean comparisons for EW vs. electrode material

on the economic costs of manufacturing the part. Thus, high rates of material removed lead to shorter machining times and therefore to a lower cost of the part. However, if the electrode wear rate was too high during the EDM process, a greater economic investment would be necessary and the part would finally be more expensive [43].

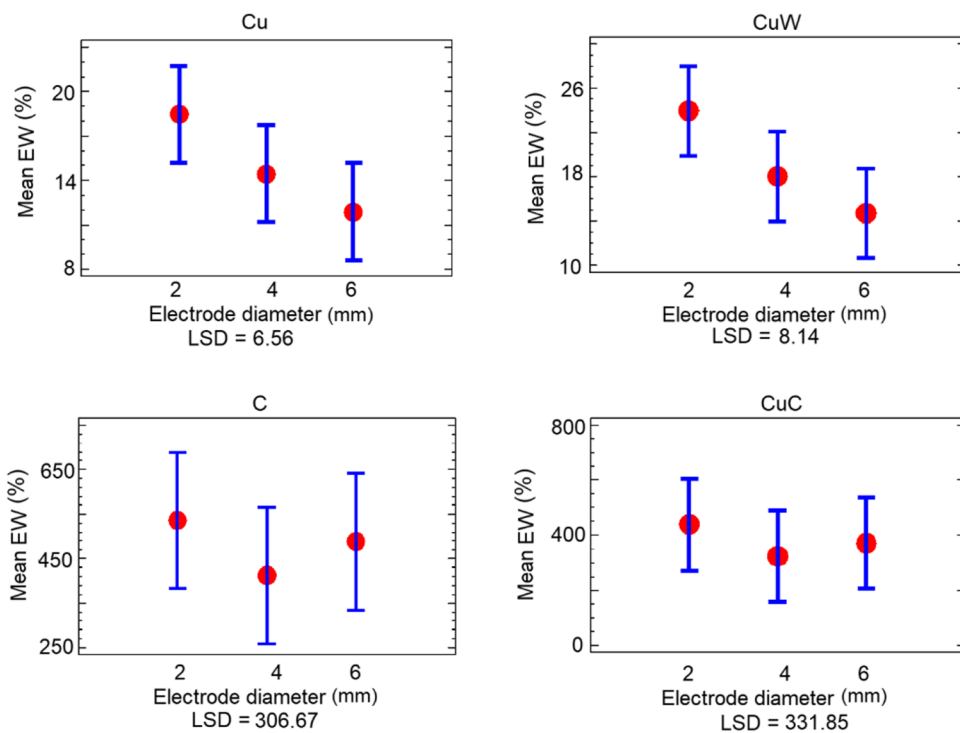
As stated in the set-up of the experimentation, negative polarity has been chosen for all the experimentation. According to the EDM process, when negative polarity is used, the negative electrons strike the surface of the positive part while the positive ions strike the surface of the negative electrode.

This continuous striking causes both the surface of the electrode and the part to melt and vaporize with each spark.

For this case study, the Cu and CuW electrodes are clearly the ones that lead to the lowest electrode wear. Likewise, similar behaviour between the Cu and CuW electrodes and between C and CuC electrodes is worth noting. As previously mentioned, this result is due to the similarity of their composition, where two groups may be distinguished: the coppers and the graphites. Moreover, it should be noted that the LSD value, represented by the total length of the interval, is the same for each case. In the case of EW, this value is 117.16.

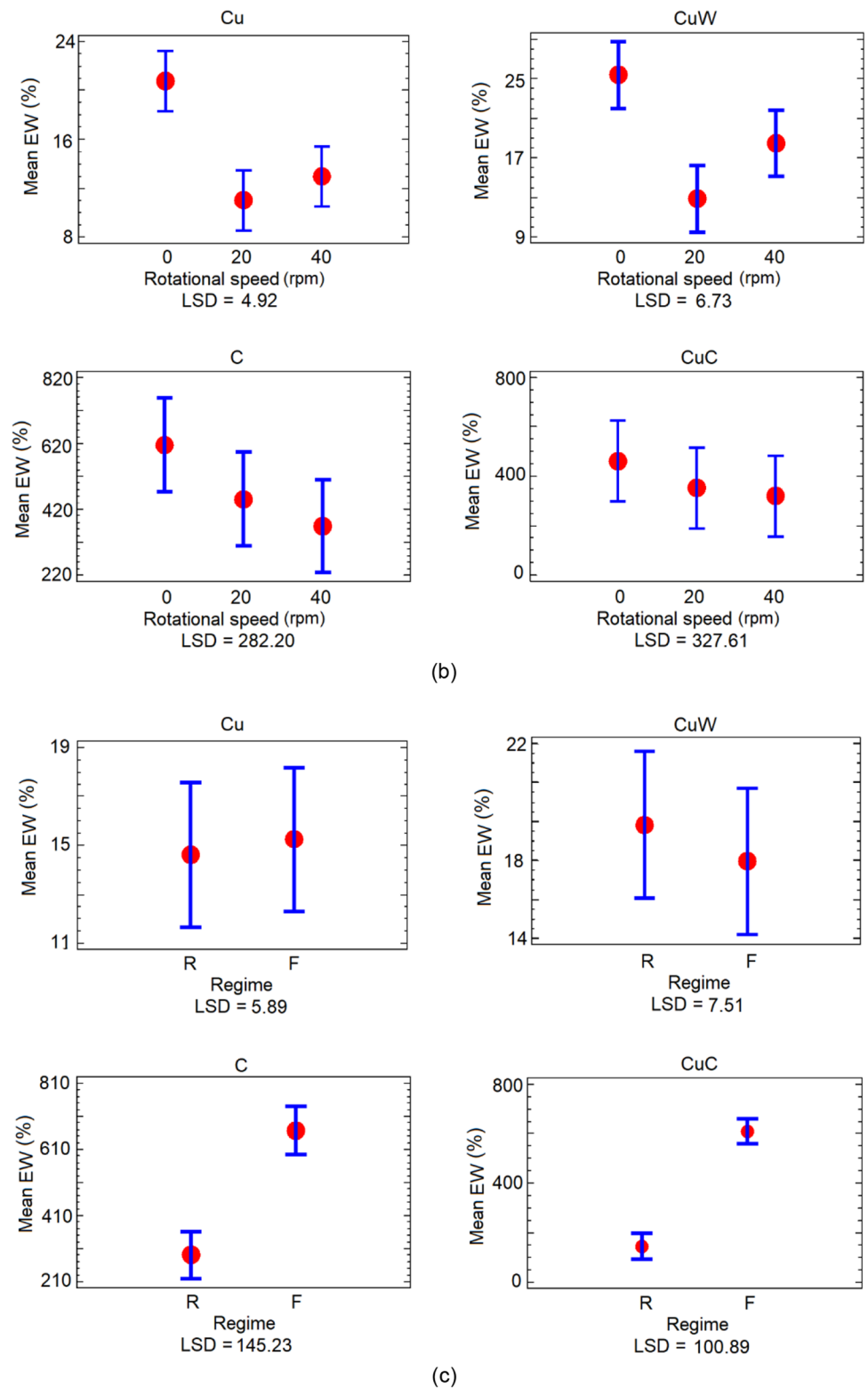
Mean comparisons between EW and parameters such as electrode diameter (a), rotational speed (b) and machining regime (c) for all the electrode materials selected are shown in Fig. 12. Similar to MRR case, the main aim of this graph is to visually identify if the influence of the factors can be considered significant in EW. As can be seen in Fig. 12(a), for Cu and CuW electrodes, the influence of the diameter is very significant when varying from 2 to 4 mm: a certain tendency to decrease wear is observed as the diameter increases in the case of both electrodes. The size of the part is larger than that of the electrode and the heat can be more easily dissipated through this part. But since the electrode is smaller, heat accumulates in it, resulting in high temperature and consequently high EW. Thus, the smaller the diameter of the electrode is, the greater its wear turns out to be.

**Fig. 12** Results for Fisher’s LSD mean comparisons for EW vs. electrode diameter (a), rotational speed (b) and machining regime (c)



(a)

Fig. 12 (continued)



In the case of rotational speed, as shown in Fig. 12(b), when C or CuC electrodes are used, the differences are not very significant either, although there is a slight tendency for the wear value to decrease with increasing rotational

speed. On the other hand, if Cu or CuW electrodes are used, there is a significant decrease in EW from 0 to 20 rpm. All these results are related to the debris cleaning. Removing the debris became increasingly easy due to the rotation of



the electrode that expelled the debris particles from the gap and improved the stability of the process, avoiding arcing and short circuits. These machining conditions result in an improvement of the EW ratio.

Meanwhile, the use of the two regimes leads to clearly different values in the case of C and CuC electrodes, where the finishing regimen leads to much higher wear values. On the contrary, in the case of Cu and CuW, the differences do not seem significant (see Fig. 12(c)).

The effect of rotational speed of a 2 mm electrode on EW at different electrode materials and machining regimes are depicted in Fig. 13. In general terms, lower electrode wears are found by using Cu and CuW electrodes compared to those obtained with C and CuC electrodes, both in finishing and roughing regimes for any electrode diameter. These results can be related to the density and the electrical resistivity of the electrodes. As Cu and CuW give the highest densification and the lowest electrical resistivity, EW tends to be lower. A high porosity induces high resistance and weak bonding between particles that drop off easily from the C and CuC electrodes. In addition, pores reduce the effective cross-sectional area and, therefore, increase the electrical resistance as it is inversely proportional to area [44].

In addition, from Fig. 13 and Table 3, it is observed that the addition of Cu in the C electrode improves the reduction of electrode wear, where this effect turns out to be greater in the case of the roughing regime. Thus, for example, in roughing regime and for the three rotational speeds selected (0, 20 and 40 rpm), values of 193.43%, 178.43% and 153.98% were achieved with CuC electrode, while values of 396.86%, 285.69% and 266.71%, respectively, were obtained with C electrode.

Regarding rotational speed of the electrode, similar behaviour can be found between the four electrode materials for both finishing and roughing regimes: as the rotational

speed increases, EW tends to decrease. This tendency is more evident for C and CuC electrodes due to the comparatively greater amount of particles suspended in the gap between the part and the electrode. Without the rotation of the electrode, cleaning is poor and suspended particles interfere with the sparks, resulting in a more unstable process.

In relation to machining regime, it should be noted in Fig. 13 that, in most cases, the greatest electrode wear was achieved in the finishing regime versus the roughing one, regardless of the rotation speed and diameter of the electrode. This fact can be attributed to the selection of the EDM machining parameters shown in Table 1. For finishing regime, in the case of Cu and CuW electrodes, a shorter pulse time was chosen whereas in the case of C and CuC electrodes, the increase in EW is due to the decrease in pause time. Due to the higher discharge frequency achieved in both cases, electrode wear was increased. Therefore, it is the increase in the number of sparks that causes greater wear and not their intensity. In other words, the number of sparks that occur at a point on the electrode surface determines the wear of the electrode, resulting in greater wear as the number of discharges (frequency) increases.

In addition, it should be noted that the difference in EW according to the regime is much more evident when C and CuC electrodes are selected. In average terms, when using a C electrode, the wear is slightly more than double in finishing regime (1006.54% at 0 rpm, 686.12% at 20 rpm and 571.79% at 40 rpm) than in the roughing one (396.86% at 0 rpm, 285.69% at 20 rpm and 266.71% at 40 rpm), for any rotational speed. In the case of the CuC electrode, this wear can increase its value up to around four times (778.83% at 0 rpm, 800.64% at 20 rpm and 607.23% at 40 rpm for roughing regime and 200.67% at 0 rpm, 178.43% at 20 rpm and 153.98% at 40 rpm in finishing regime, respectively).

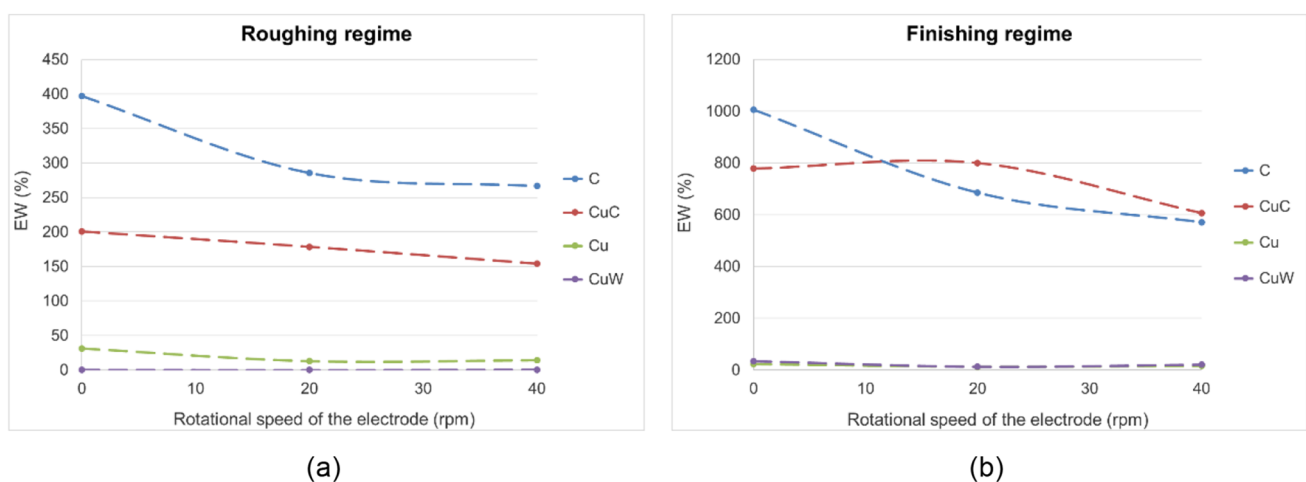


Fig. 13 Effect of rotational speed on EW at different electrode materials and working conditions (electrode diameter 2 mm)

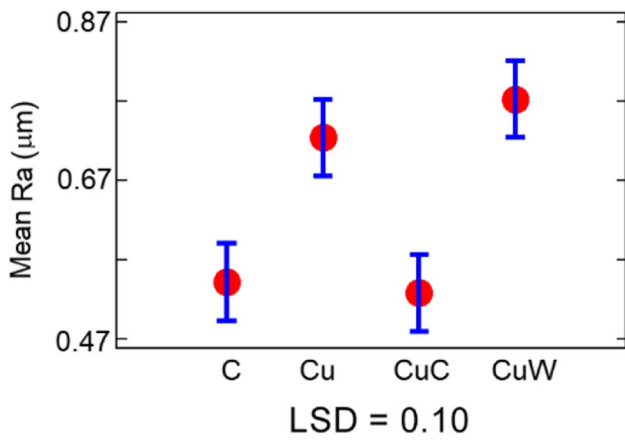


Fig. 14 Results for Fisher’s LSD mean comparisons for Ra vs. electrode material

### 5.3 Surface roughness

Regarding surface roughness, similar results were found to those obtained for MRR, as can be appreciated in Fig. 14 that relates Ra roughness parameter and electrode material. Moreover, it should be noted that the LSD value is 0.10.

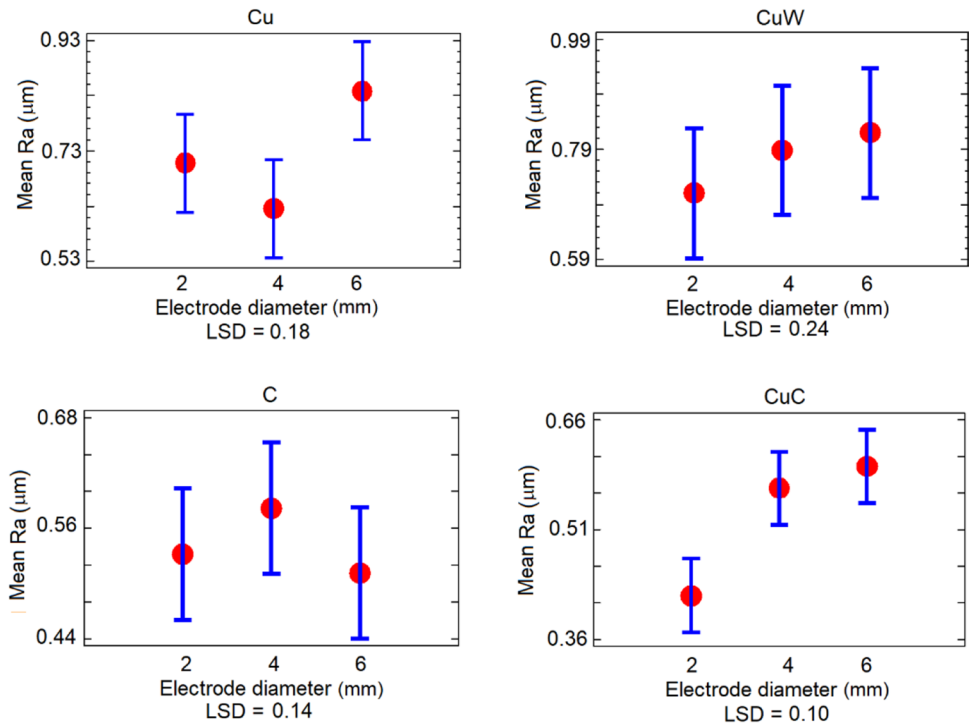
In general, EDM’ed surfaces are characterized by non-directional and spherical discharge cavities. The size of these cavities depends on the melting temperature of the materials selected, the electrical power of each spark and

its duration. In this study case, Cu and CuW electrodes produced the roughest surfaces whereas the smoothest surfaces were found when C and CuC electrodes were used. This is mainly due to two factors: on the one hand, because of the fact that Cu and CuW materials have a low melting temperature and some material from the electrode was removed for each spark. The resulting irregularities on the electrode surface are copied onto the part surface in the form of larger peaks and valleys. On the other hand, the lower electrical resistivity of Cu and CuW to that of C and CuC leads to a more stable and homogeneous process. Thus, more material is removed from the part and the resulting surface worsens. The irregularities and cavities produced by the energetic sparks are considerably greater, leaving a rougher surface.

In addition, in order to identify if there are any significant differences between the four electrode materials selected in this study. Figure 15 shows a summary plot of Ra mean data of each material as a function of electrode diameter (a), rotational speed of the electrode (b), and machining regime (c). As can be seen, the variation in diameter has little influence on Ra, with no significant differences being observed in the case of C and CuW. In the case of Cu electrode, significant differences can be appreciated between diameters of 2 and 3 mm with respect to that of 4 mm whereas for CuC electrode, the greatest influence is observed when the diameter is 2 mm.

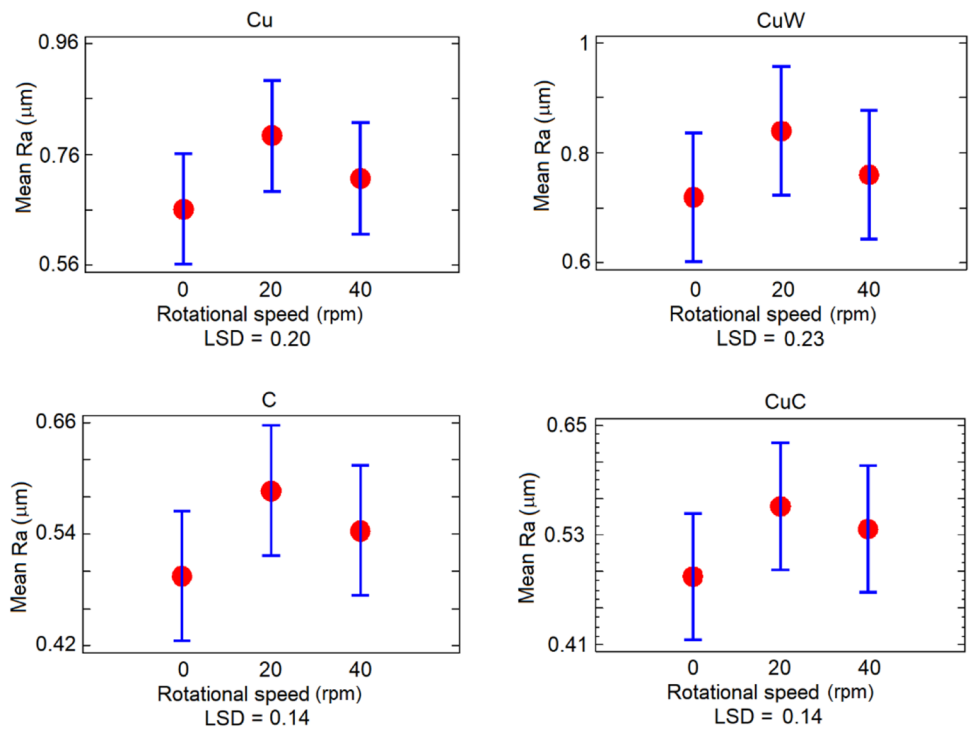
In the case of the rotational speed of the electrode, from 10 to 40 rpm, the differences are not significant either, with the

Fig. 15 Results for Fisher’s LSD mean comparisons for Ra vs. electrode diameter (a), rotational speed (b) and machining regime (c)

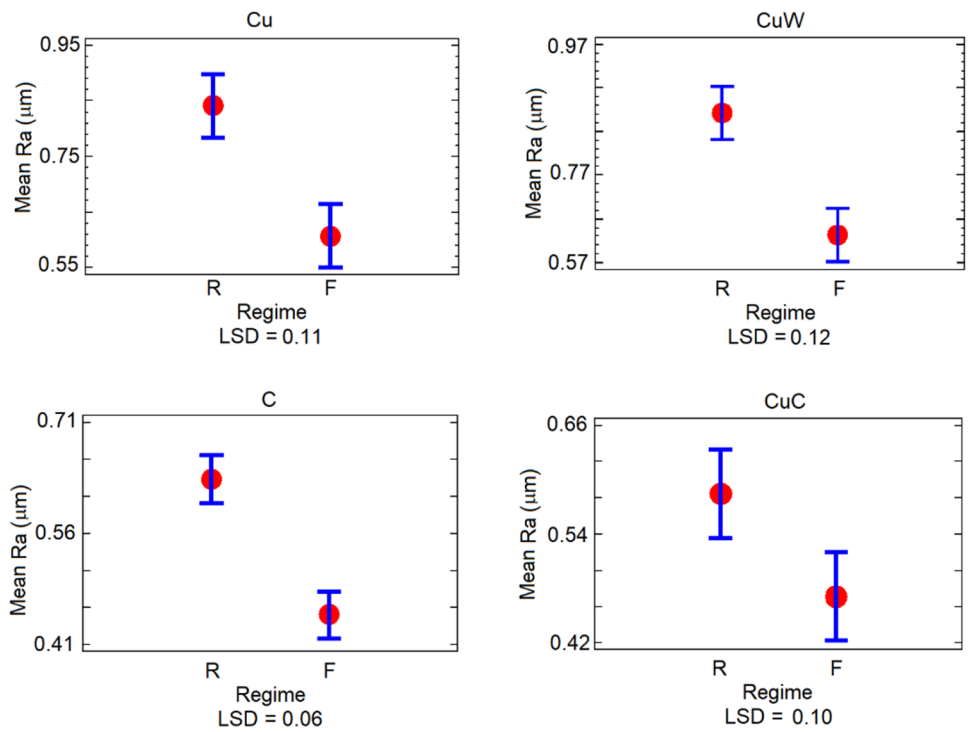


(a)

Fig. 15 (continued)



(b)



(c)

lowest values of surface roughness always being obtained when the electrode does not rotate. Finally, it can be seen that great differences in Ra for all electrode materials occur where the finishing regime always results in a better surface finish relative to the roughing one.

Regarding surface roughness depending on the electrode material, similar trends can be seen between Cu and CuW electrodes and C and CuC electrodes, respectively as shown in Fig. 16. Likewise, in roughing regime, the highest Ra values were obtained with Cu and CuW electrodes,

for any electrode diameter as can be observed in Table 4. This is mainly due to the machining parameters selected. For both materials, the longer the pulse time, the higher the roughness. By increasing the pulse time, the plasma channel expands which allows the discharge energy to be increased. In other words, long pulses mean a large quantity of energy transferred to the material, which produces deeper craters and larger irregularities during this time. Whereas at low discharge energy, the craters are less evident and less frequent and therefore their shape is smooth and shallow.

In fact, the greatest differences in Ra values are found when varying the machining regime and the electrode material and they are slightly lower when varying the rotation of the electrode. Experimental results show the lowest values of Ra when there is no rotation of the electrode while at 20 rpm the resulting EDM surface worsens. This can be explained by the fact that at 0 rpm, time machining is too high. However, it should be noted that, in most experiments, Ra values at 40 rpm are very close to those obtained at 0 rpm. This means that higher values than 40 rpm are necessary, at a minimum, in order to provide a thorough flushing debris in the gap. Thus, the recast layer on the machined surface was more washed off.

With Cu and CuW electrodes, both in finishing and roughing regimes, the highest values of Ra are 1.07  $\mu\text{m}$  and 1.11  $\mu\text{m}$ , respectively, and are found at 20 rpm. In such cases, the surface roughness increases with increasing rotational speed up to a maximum (20 rpm), after which it begins to decrease.

In general terms, in the roughing regime, for any material and electrode diameter, the highest Ra values are obtained at 20 rpm (only exception: 4 mm diameter copper electrode: at 20 rpm, Ra=0.98  $\mu\text{m}$  and at 40 rpm, Ra=1.07  $\mu\text{m}$ ,

where the difference is minimal). Meanwhile, in the finishing regime, for any electrode diameter, the highest Ra is obtained at 20 rpm with Cu and CuW electrodes, and at 40 rpm with C and CuC electrodes. So, finish surface roughness could be obtained by setting low current intensity values combined with CuC or C electrodes, although this approach is more time-consuming.

All these results and tendencies agree with those obtained for MRR, except for the C electrode results. In this case, some slight differences were found but they are not significantly relevant. Thus, it was observed that selecting roughing regime always leads to higher removal rates and higher Ra values on any of the four electrode materials experimented and vice versa.

Figure 17(a) and (b) shows the electrode entry hole of the experiment E14\_CuW corresponding to the maximum value of Ra (1.11  $\mu\text{m}$ ) and of the experiment E4\_C corresponding to the minimum Ra value (0.37  $\mu\text{m}$ ), respectively. As previously mentioned, these values can be found in Table 4 and were obtained by using a profile rugosimeter. Furthermore, it should be stated that both surfaces were also measured with the microscope and, in this case, Ra values were 1.08  $\mu\text{m}$  for E14\_CuW and 0.47  $\mu\text{m}$  for E4\_C. As can be seen, both results are very similar.

According to Fig. 17, in both cases, the shape of the hole is well defined and the edges can be clearly seen. In addition, the surface appears homogeneous and flat and re-solidified particles are not appreciated round about because of the efficient debris cleaning. Thus, the high flow velocity of the dielectric fluid caused hydraulic forces that ejected the molten material radially away.

The quality of holes produced with EDM depends mainly on the material of the electrode but also on the energy of discharges applied during the machining process.

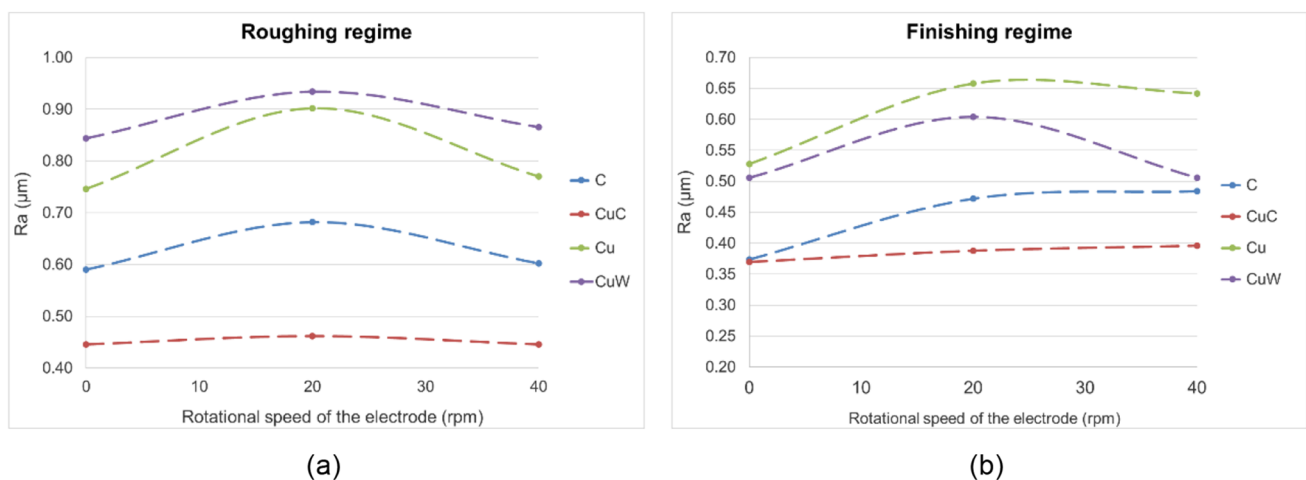
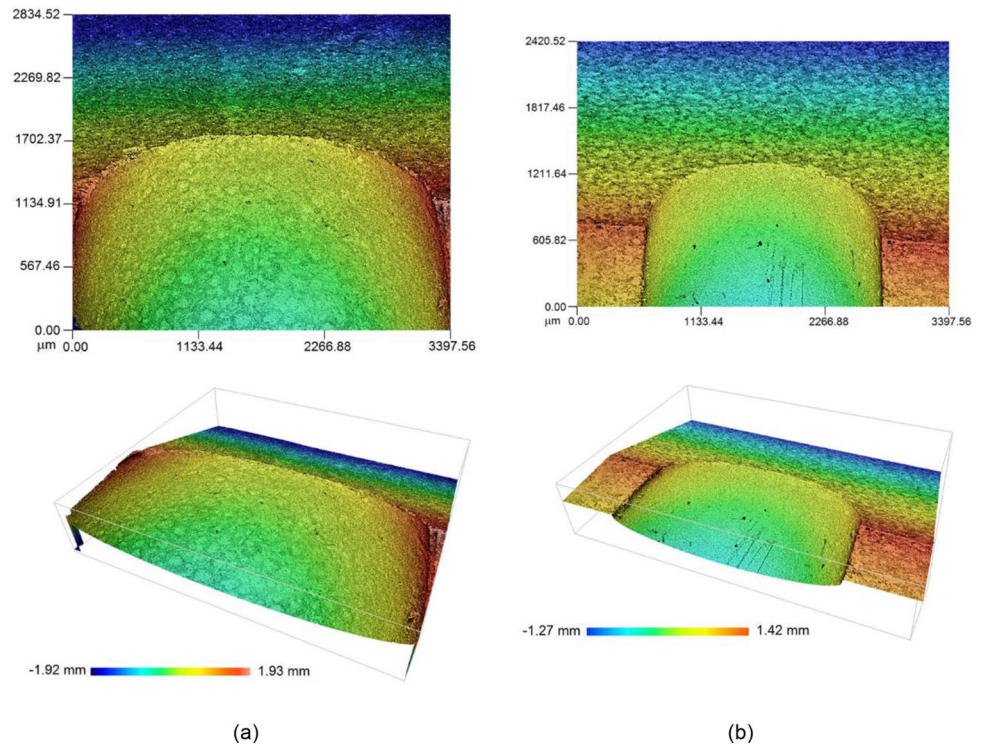


**Fig. 16** Effect of rotational speed on Ra at different electrode materials and working conditions (electrode diameter 2 mm)



**Fig. 17** Surface topography at the entrance of the hole at (a) maximum Ra (E14\_CuW) and (b) minimum Ra (E4\_C) conditions



Experimental results reveal the highest Ra values in the roughing regime versus the finishing regime. As current intensity is higher in roughing regime, thermal energy is increased and the surface of the SiSiC ceramic is clearly affected. Consequently, more molten material from the piece is produced whereas flushing debris by the dielectric fluid becomes more difficult, and the resulting recast layer worsens the surface finish [21]. As current intensity is decreased, sparks are less energetic and the EDM’ed surface is less damaged and more uniform. Therefore, low Ra and MRR values are attained.

Finally, in order to conclude this section, Table 7 summarizes the results previously discussed in this present study. As can be observed, the most influential factors are included.

### 6 Conclusions

This present study deals with the machining of through holes on SiSiC advanced ceramic by using EDM drilling technology. The influence of electrode material, electrode diameter, rotational speed of the electrode and the machining regime on EDM performance as well as surface roughness was investigated profoundly. The following conclusions may be drawn up:

- From the experimental results, both electrode material and machining regime seem to be the most relevant factors of all. Moreover, results for C and CuC electrodes are found to be similar in terms of machining speed, elec-

**Table 7** Main results

	MRR (mm <sup>3</sup> /min)		EW (%)		Ra (μm)	
	Max	Min	Max	Min	Max	Min
Values	0.4974	0.0206	1006.54	7.52	1.11	0.37
Electrode material	CuW	C	C	Cu	CuW	C
Electrode diameter (mm)	3	2	2	4	4	2
Rotational speed (rpm)	20	0	0	20	20	0
Regime (machining conditions)	Roughing ( <i>I</i> =2 A; <i>t<sub>i</sub></i> =70 μs; <i>η</i> =0.6)	Finishing ( <i>I</i> =0.5 A; <i>t<sub>i</sub></i> =50 μs; <i>η</i> =0.6)	Finishing ( <i>I</i> =0.5 A; <i>t<sub>i</sub></i> =50 μs; <i>η</i> =0.6)	Roughing ( <i>I</i> =2 A; <i>t<sub>i</sub></i> =70 μs; <i>η</i> =0.6)	Roughing ( <i>I</i> =2 A; <i>t<sub>i</sub></i> =70 μs; <i>η</i> =0.6)	Finishing ( <i>I</i> =0.5 A; <i>t<sub>i</sub></i> =50 μs; <i>η</i> =0.6)

trode wear and surface finish. However, there are significant differences between the results of the two previous materials and those of Cu and CuW, which, in turn, constitute homogeneous groups between them.

- The use of Cu and CuW electrodes led to the highest values of MRR and Ra but the lowest values of EW compared to those obtained with C and CuC electrodes, both in finishing and roughing regimes for any electrode diameter. Specifically, in roughing regime and at 20 rpm, the greatest removal rate is appreciated, whatever the diameter of the electrode.
- Experimental results indicate that the highest value of MRR is  $0.4974 \text{ mm}^3/\text{min}$  and it was obtained with a CuW electrode and a rotational speed of 20 rpm while the lowest EW value is 7.52% and it was obtained with a Cu electrode and at 20 rpm. Moreover, both experiments were performed to 2 A and a pulse time value of  $70 \mu\text{m}$ .
- Since the rotational speed of the electrode does not have a great influence on the machinability and surface finish of the part, some results must be explained. In general, the highest rates of material removal were achieved by rotating the electrode as a consequence of a better debris evacuation. For the same reason, it was found that a decreasing in EW takes place as the rotational speed of the electrode increases. Indeed, this tendency becomes even clearer for C and CuC electrodes due to the comparatively greater amount of particles suspended in the gap. Regarding Ra, in most cases, similar results were achieved at 0 rpm and 40 rpm. In the first case, Ra was low as a result of a too-high-time machining while at 40 rpm the cleaning in the gap was enough to evacuate all the debris particles. Thus, the lowest value of Ra is  $0.37 \mu\text{m}$  and was obtained with a C electrode and with no electrode rotation whereas at 40 rpm and, under the same conditions, Ra value is  $0.40 \mu\text{m}$ . However, comparing MRR values for both experiments, at 40 rpm the removal rate was doubled and time machining was reduced by more than half.
- With regard to machining regime, experimental results reveal the highest values of MRR and Ra in the roughing regime versus the finishing one.
- For the materials and parameters under consideration in the present study, it has been found that the copper electrode rotating at 20 rpm combined with high values of discharge energy is the most economical option in terms of production cost and production time, as it gives the highest values of MRR and the lowest electrode wear. However, a finish surface roughness could be obtained by setting low current intensity values combined with CuC or C electrodes, although this approach is more time-consuming. In addition, it may be observed that the addition of Cu in the C electrode contributes to a greater removal of material and slightly reduces the wear of the electrode.

**Funding** Open Access funding provided by Universidad Pública de Navarra.

**Data availability** The experimental results necessary to reproduce all analyses are provided in the manuscript.

## Declarations

**Ethics approval** The submitted manuscript is original, complete and has not been submitted/published elsewhere in any form or language.

**Consent to participate** All the authors voluntarily agree to participate in this research study.

**Consent for publication** All the authors consent to the publication of the manuscript in *The International Journal of Advanced Manufacturing Technology*.

**Conflict of interest** The authors declare no competing interests.

**Open Access** This article is licensed under a Creative Commons Attribution 4.0 International License, which permits use, sharing, adaptation, distribution and reproduction in any medium or format, as long as you give appropriate credit to the original author(s) and the source, provide a link to the Creative Commons licence, and indicate if changes were made. The images or other third party material in this article are included in the article's Creative Commons licence, unless indicated otherwise in a credit line to the material. If material is not included in the article's Creative Commons licence and your intended use is not permitted by statutory regulation or exceeds the permitted use, you will need to obtain permission directly from the copyright holder. To view a copy of this licence, visit <http://creativecommons.org/licenses/by/4.0/>.

## References

1. Kliuev M, Maradia U, Wegener K (2018) EDM drilling of non-conducting materials in deionised water. *Procedia CIRP* 68:11–16. <https://doi.org/10.1016/j.procir.2017.12.014>
2. Skrabalak G (2018) Influence of electrode tool length on the micro EDM drilling performance. *Procedia CIRP* 68:594–598. <https://doi.org/10.1016/j.procir.2017.12.120>
3. Rahman MZ, Das AK, Chattopadhyaya S (2018) Comparative studies in electro-physical processes (ECM & EDM) for circular micro-holes drilling. *Mater Today: Proc* 5:27690–27699. <https://doi.org/10.1016/j.matpr.2018.10.003>
4. Chaudhury P, Samantaray S (2021) A comparative study of different dielectric medium for sustainable EDM of non-conductive material by electro-thermal modelling. *Mater Today: Proc* 41:437–444. <https://doi.org/10.1016/j.matpr.2020.10.162>
5. Hammel EC, Ighodaro OLR, Okoli OI (2014) Processing and properties of advanced porous ceramics: an application based review. *Ceram Int* 40(10):15351–15370. <https://doi.org/10.1016/j.ceramint.2014.06.095>
6. Farooqui MN, Patil NG (2018) A perspective on shaping of advanced ceramics by electro discharge machining. *Procedia Manuf* 20:65–72. <https://doi.org/10.1016/j.promfg.2018.02.009>
7. Keller AR, Zhou M (2003) Effect of microstructure on dynamic failure resistance of titanium diboride/alumina ceramics. *J Am Ceram Soc* 86(3):449–457. <https://doi.org/10.1111/j.1151-2916.2003.tb03320.x>

8. Szutkowska M, Boniecki M (2006) Subcritical crack growth in zirconia-toughened alumina (ZTA) ceramics. *J Mater Process Technol* 175(1–3):416–420. <https://doi.org/10.1016/j.jmatprotec.2005.04.030>
9. Ming W, Jia H, Zhang H, Zhang Z, Liu K, Du J, Shen F, Zhang G (2020) A comprehensive review of electric discharge machining of advanced ceramics. *Ceram Int* 46:21813–21838. <https://doi.org/10.1016/j.ceramint.2020.05.207>
10. López de la Calle LN, Pérez J, Llorente JI, Sánchez JA (2000) Advanced cutting conditions for the milling of aeronautical alloys. *J Mater Process Technol* 100:1–11. [https://doi.org/10.1016/S0924-0136\(99\)00372-6](https://doi.org/10.1016/S0924-0136(99)00372-6)
11. Bilal A, Jahan MP, Talamona D, Perveen A (2019) Electrodischarge machining of ceramics: a review. *Micromachines* 10. <https://doi.org/10.3390/mi10010010>
12. Mahdavinejad RA, Mahdavinejad A (2005) ED machining of WC-Co. *J Mater Process Technol* 162–163:637–643. <https://doi.org/10.1016/j.jmatprotec.2005.02.211>
13. Schubert A, Zeidler H, Kühn R, Hackert-Oschätzchen M (2015) Microelectrical discharge machining: a suitable process for machining ceramics. *J Ceram*. <https://doi.org/10.1155/2015/470801>
14. Clijsters S, Liu K, Reynaerts D, Lauwers B (2010) EDM technology and strategy development for the manufacturing of complex parts in SiSiC. *J Mater Process Technol* 210:631–641. <https://doi.org/10.1016/j.jmatprotec.2009.11.012>
15. Wei C, Zhao L, Hu D, Ni J (2013) Electrical discharge machining of ceramic matrix composites with ceramic fiber reinforcements. *Int J Adv Manuf Technol* 64:187–194. <https://doi.org/10.1007/s00170-012-3995-5>
16. Daud ND, MohdGhazali FA, Abd Hamid FK, Nafea M, Saleh T, Leow PL, Mohamed Ali MS (2021) Heat-assisted  $\mu$ -electrical discharge machining of silicon. *Int J Adv Manuf Technol* 113:1727–1738. <https://doi.org/10.1007/s00170-021-06734-y>
17. Saleh T, Rasheed AN, Muthalif AGA (2015) Experimental study on improving  $\mu$ -WEDM and  $\mu$ -EDM of doped silicon by temporary metallic coating. *Int J Adv Manuf Technol* 78:1651–1663. <https://doi.org/10.1007/s00170-014-6732-4>
18. Lauwers B, Kruth JP, Liu W, Eeraerts W, Schacht B, Bleys P (2004) Investigation of material removal mechanisms in EDM of composite ceramic materials. *J Mater Process Technol* 149:347–352. <https://doi.org/10.1016/j.jmatprotec.2004.02.013>
19. D'Urso G, Maccarini G, Ravasio C (2016) Influence of electrode material in micro-EDM drilling of stainless steel and tungsten carbide. *Int J Adv Manuf Technol* 85:2013–2025. <https://doi.org/10.1007/s00170-015-7010-9>
20. Yongfeng G, Yerui F, Li W, Kelie D, Changjin M, Lin T (2018) Experimental investigation of EDM parameters for ZrB<sub>2</sub>-SiC ceramics machining. *Procedia CIRP* 68:46–51. <https://doi.org/10.1016/j.procir.2017.12.020>
21. Guu H, Hocheng H (2001) Effects of workpiece rotation on machinability during electrical discharge machining. *Mater Manuf Process* 16(1):91–101. <https://doi.org/10.1081/AMP-100103699>
22. Kliuev M, Maradia U, Boccadoro M, Perez R, Stirnimann J, Wegener K (2016) Experimental study of EDM-drilling and shaping of SiSiC and SiC. *Procedia CIRP* 42:191–196. <https://doi.org/10.1016/j.procir.2016.02.269>
23. Ji R, Liu Y, Zhang Y, Wang F (2011) Machining performance of silicon carbide ceramic in end electric discharge milling. *Int J Refrac Metal Hard Mater* 29:117–122. <https://doi.org/10.1016/j.jrmhm.2010.09.001>
24. Gao Q (2018) Impact of electrode length on EDM inclined hole drilling process. *Int J Adv Manuf Technol* 94:1171–1175. <https://doi.org/10.1007/s00170-017-0937-2>
25. Li H, Wang Z, Wang Y, Liu H, Bai Y (2017) Micro-EDM drilling of ZrB<sub>2</sub>-SiC-graphite composite using micro sheet-cylinder tool electrode. *Int J Adv Manuf Technol* 92:2033–2041. <https://doi.org/10.1007/s00170-017-0296-z>
26. Risto M, Haas R, Munz M (2016) Optimization of the EDM drilling process to increase the productivity and geometrical accuracy. *Procedia CIRP* 42:537–542. <https://doi.org/10.1016/j.procir.2016.02.247>
27. Diver C, Atkinson J, Helml HJ, Lib L (2004) Micro-EDM drilling of tapered holes for industrial applications. *J Mater Process Technol* 149:296–303. <https://doi.org/10.1016/j.jmatprotec.2003.10.064>
28. Bamberg E, Heamawatanachai S (2009) Orbital electrode actuation to improve efficiency of drilling micro-holes by micro-EDM. *J Mater Process Technol* 209:1826–1834. <https://doi.org/10.1016/j.jmatprotec.2008.04.044>
29. Yamazaki M, Suzuki T, Mori N, Kunieda M (2004) EDM of micro-rods by self-drilled holes. *J Mater Process Technol* 149:134–138. <https://doi.org/10.1016/j.jmatprotec.2004.03.006>
30. Tanjilul M, Ahmed A, Senthil Kumar A, Rahman M (2018) A study on EDM debris particle size and flushing mechanism for efficient debris removal in EDM-drilling of Inconel 718. *J Mater Process Technol* 255:263–274. <https://doi.org/10.1016/j.jmatprotec.2017.12.016>
31. Li C, Zhang B, Li Y, Tonga H, Ding S, Wang Z, Zhao L (2018) Self-adjusting EDM/ECM high speed drilling of film cooling holes. *J Mater Process Technol* 262:95–103. <https://doi.org/10.1016/j.jmatprotec.2018.06.026>
32. Luis CJ, Puertas I (2007) Methodology for developing technological tables used in EDM processes of conductive ceramics. *J Mater Process Technol* 189:301–309. <https://doi.org/10.1016/j.jmatprotec.2007.01.041>
33. Baghel R, Mali HS, Biswas SK (2019) Parametric optimization and surface analysis of diamond grinding-assisted EDM of TiN-Al<sub>2</sub>O<sub>3</sub> ceramic composite. *Int J Adv Manuf Technol* 100:1183–1192. <https://doi.org/10.1007/s00170-018-1842-z>
34. Luis CJ, Puertas I, Villa G (2005) Material removal rate and electrode wear study on the EDM of silicon carbide. *J Mater Process Technol* 164:889–896. <https://doi.org/10.1016/j.jmatprotec.2005.02.045>
35. UNE-EN ISO 4287:1999 (1999) Geometrical product specifications (GPS) – surface texture: profile method – terms, definitions and surface texture parameters. AENOR, Madrid
36. Sánchez JA, Cabanes I, López de la Calle LN, Lamikiz A (2001) Development of optimum electrodischarge machining technology for advanced ceramics. *Int J Adv Manuf Technol* 18:897–905. <https://doi.org/10.1007/PL00003958>
37. Montgomery DC (2001) Design and analysis of experiments. Wiley, New York
38. Wang K, Zhang Q, Zhu G, Huang Y, Zhang J (2018) Influence of tool size on machining characteristics of micro-EDM. *Procedia CIRP* 68:604–609. <https://doi.org/10.1016/j.procir.2017.12.122>
39. Liu Q, Zhang Q, Zhu G, Wang K, Zhang J, Dong C (2016) Effect of electrode size on the performances of micro-EDM. *Mater Manuf Process* 31(4):391–396. <https://doi.org/10.1080/10426914.2015.1059448>
40. Jameson EC (2001) Electrical discharge machining. Society of Manufacturing Engineers, Michigan

41. Khan AA (2008) Electrode wear and material removal rate during EDM of aluminum and mild steel using copper and brass electrodes. *Int J Adv Manuf Technol* 39:482–487. <https://doi.org/10.1007/s00170-007-1241-3>
42. Munz M, Risto M, Haas R (2013) Specifics of flushing in electrical discharge drilling. *Procedia CIRP* 6:83–88. <https://doi.org/10.1016/j.procir.2013.03.024>
43. Torres A, Puertas I, Luis CJ (2016) EDM machinability and surface roughness analysis of INCONEL 600 using graphite electrodes. *Int J Adv Manuf Technol* 84:2671–2688. <https://doi.org/10.1007/s00170-015-7880-x>
44. Li L, Wong YS, Fuh JYH, Lu L (2001) Effect of TiC in copper-tungsten electrodes on EDM performance. *J Mater Process Technol* 113:563–567. [https://doi.org/10.1016/S0924-0136\(01\)00622-7](https://doi.org/10.1016/S0924-0136(01)00622-7)

**Publisher's Note** Springer Nature remains neutral with regard to jurisdictional claims in published maps and institutional affiliations.